Dispersion of Nanoparticles Using Twin Screw Extrusion Technologies; Challenges and Opportunities

Dilhan Kalyon/Seher Ozkan/Halil Gevgilili/
Jim Kowalczyk*
Stevens Institute of Technology
* Material Processing & Research Inc.

Figure 1

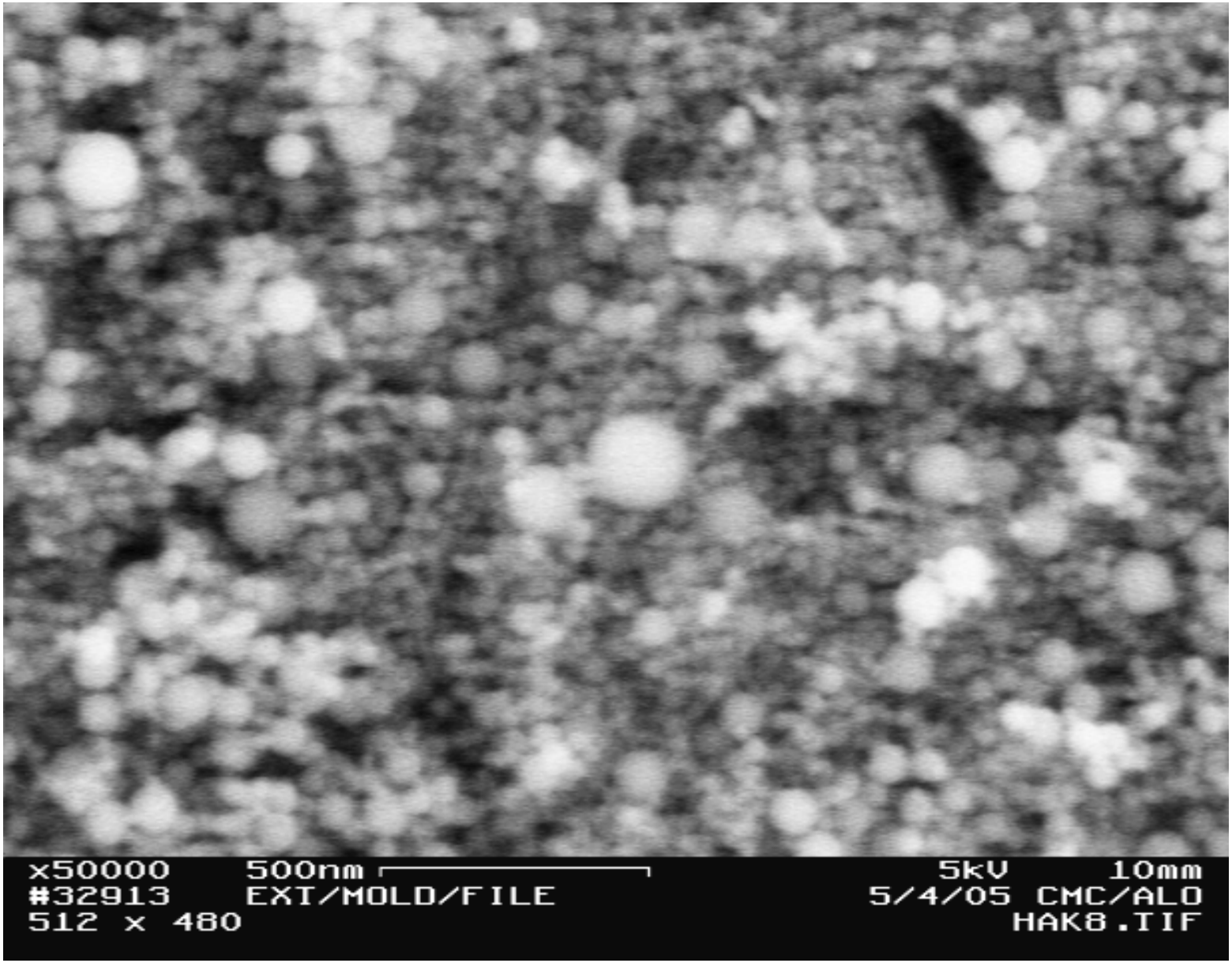

γ-Al_2O_3 Particles.

Figure 2

(Inframat Avanced Materials, LLC, CT., USA. Particle size 40nm)

Co-rotating twin screw extruder:

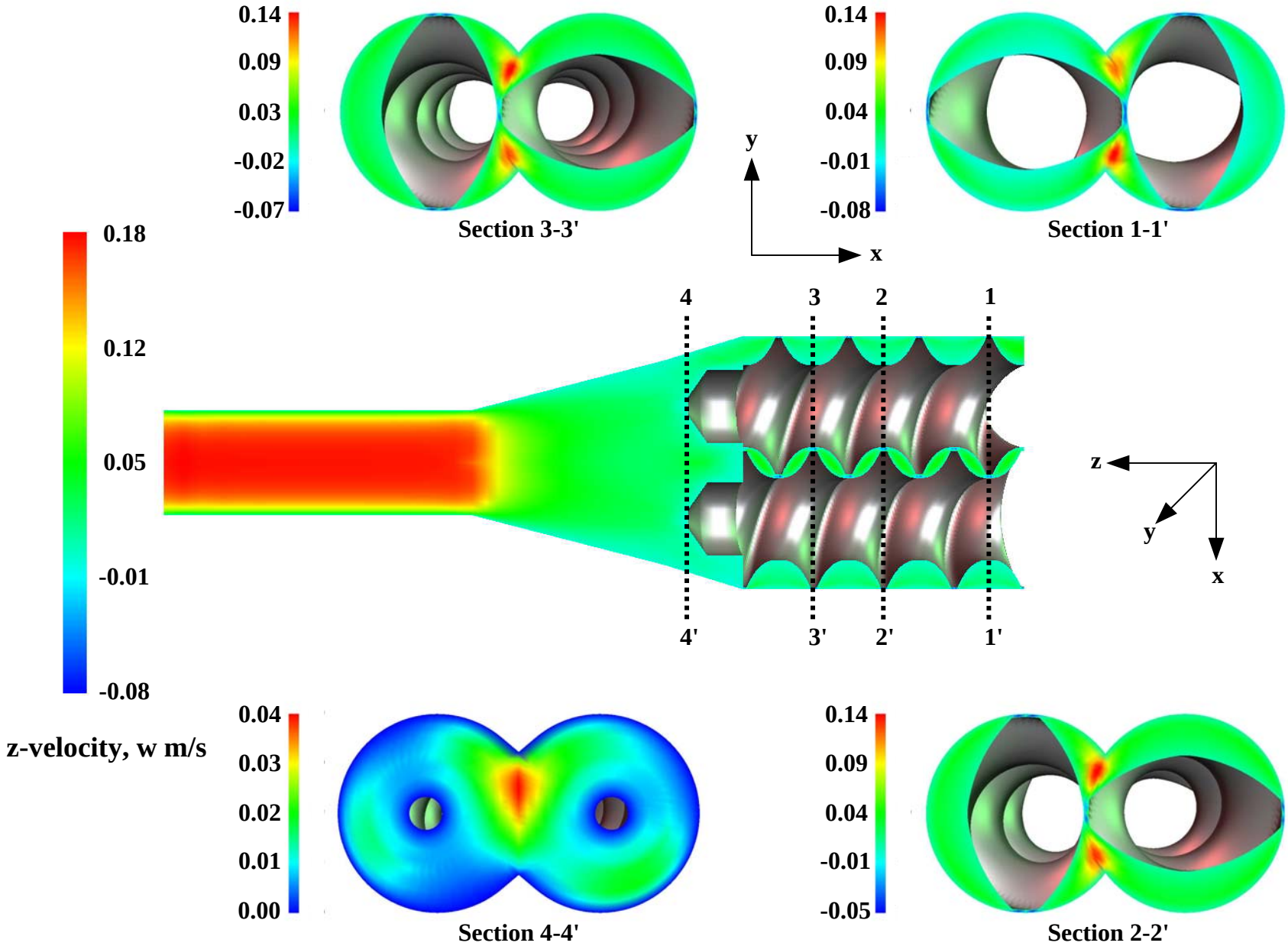

Comparisons of mixing characteristics

- Co-rotating twin screw extrusion
- Counter-rotating twin screw extrusion
- Batch mixing (mini Banbury mixer) for benchmarking
- USE: Conductive composite, with Kraton binder and conductive graphite particles

Figure 4

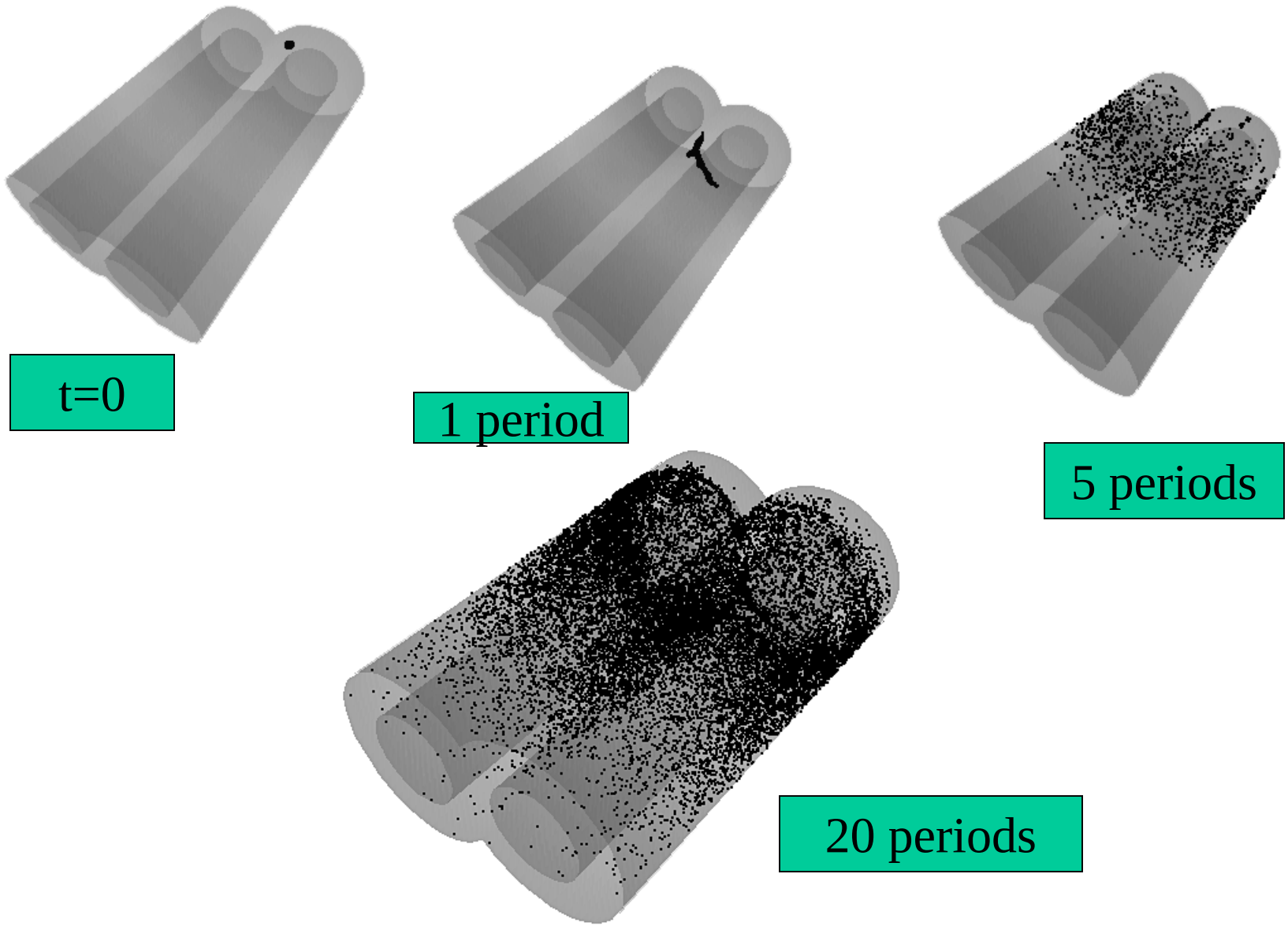

Analysis of Kneading Disks staggered at 30 forward

Figure 5

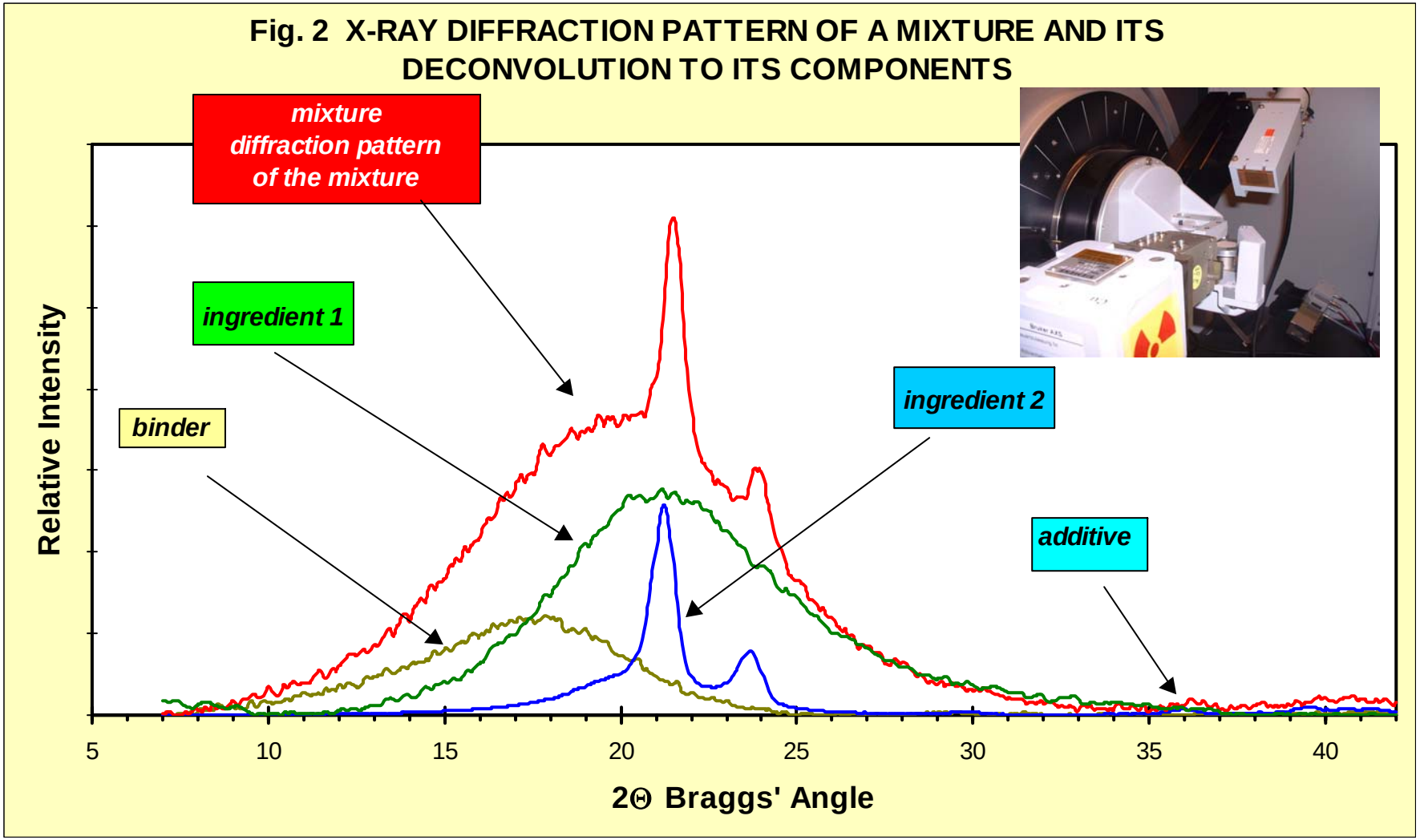
Fig. 2 X-RAY DIFFRACTION PATTERN OF A MIXTURE AND ITS DECONVOLUTION TO ITS COMPONENTS
mixture diffraction pattern of the mixture
ingredient 1
binder
ingredient 2
additive
Relative Intensity
5
10
15
20
25
30
35
40
2Θ Braggs' Angle

Figure 6

$$s^2 \quad \frac{1}{(N \quad 1)} \quad {}_{i \ 1}^{N} \quad c_i \quad \bar{c}^{\,2}$$

S is the standard deviation, C_i is the concentration,
$\bar{C}$ is the average, N is the number of specimens

Figure 7

$$s_0^2 \quad \bar{c}(1 \quad \bar{c})$$

Variance for the completely segregated sample

Figure 8

<u>Mixing Index</u> for concentration distributions,

<u>MI</u> = 1 – s/s$_o$

Figure 9

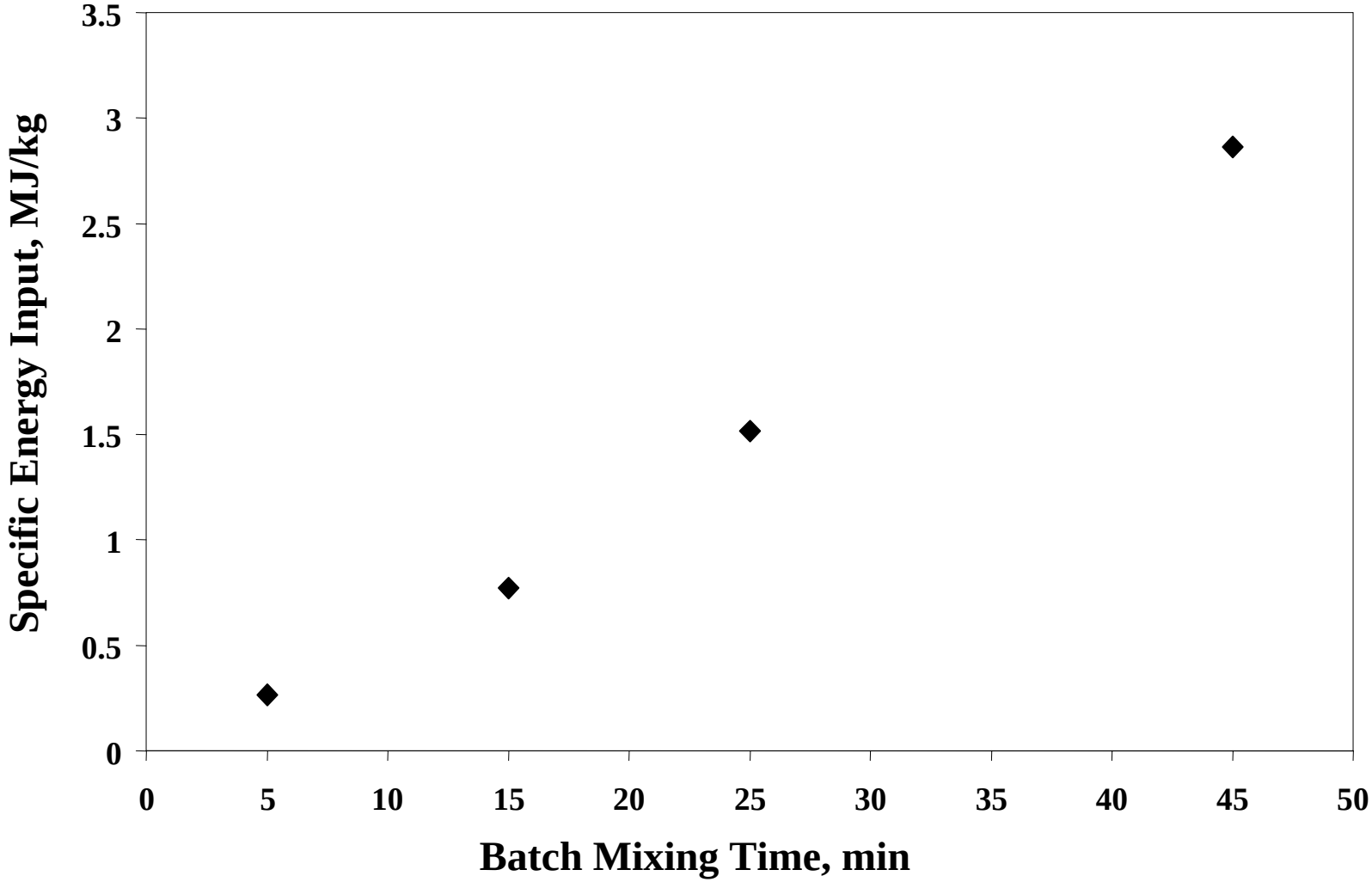

Specific energy input as a function of batch mixing time: Example with graphite loading

Figure 10

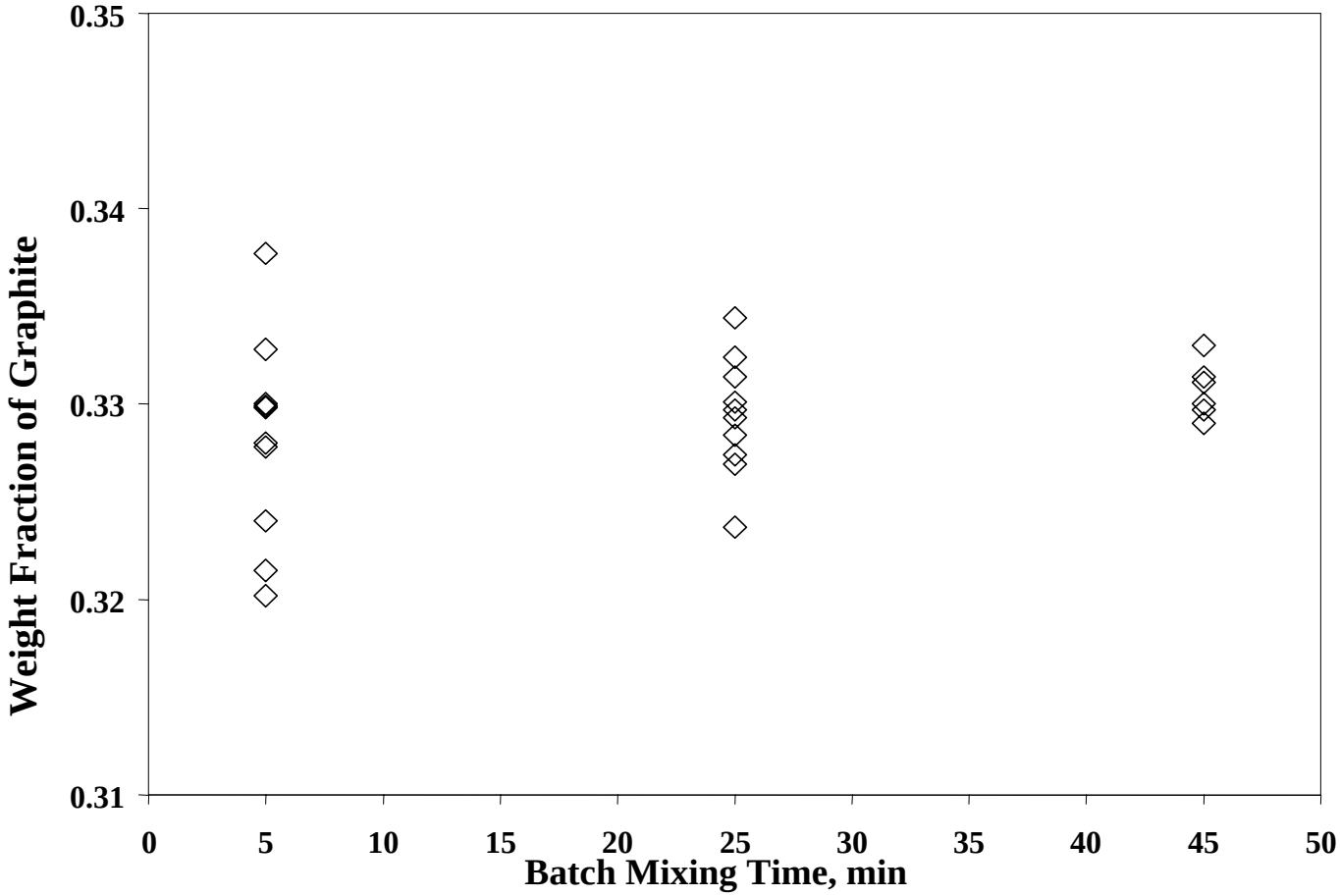

Weight fraction of graphite obtained from TGA experiments for batch-mixed specimens

Example with graphite loading

Figure 11

The use of co-rotating twin screw extrusion

Nanoparticles of alumina to be processed into CMC gel (simulant for nitrocellulose based systems), use batch mixing for benchmarking

Figure 12

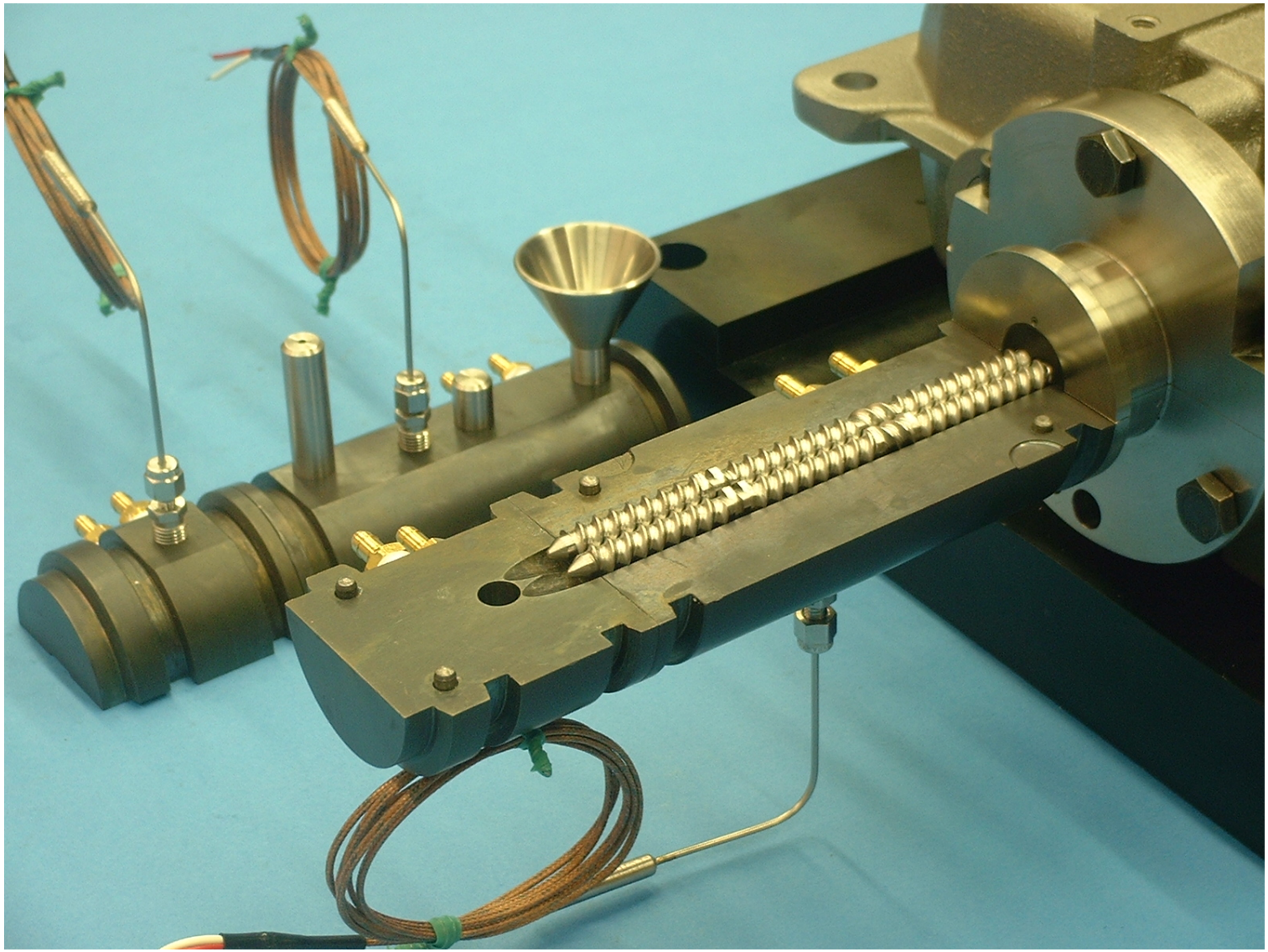

Figure 13

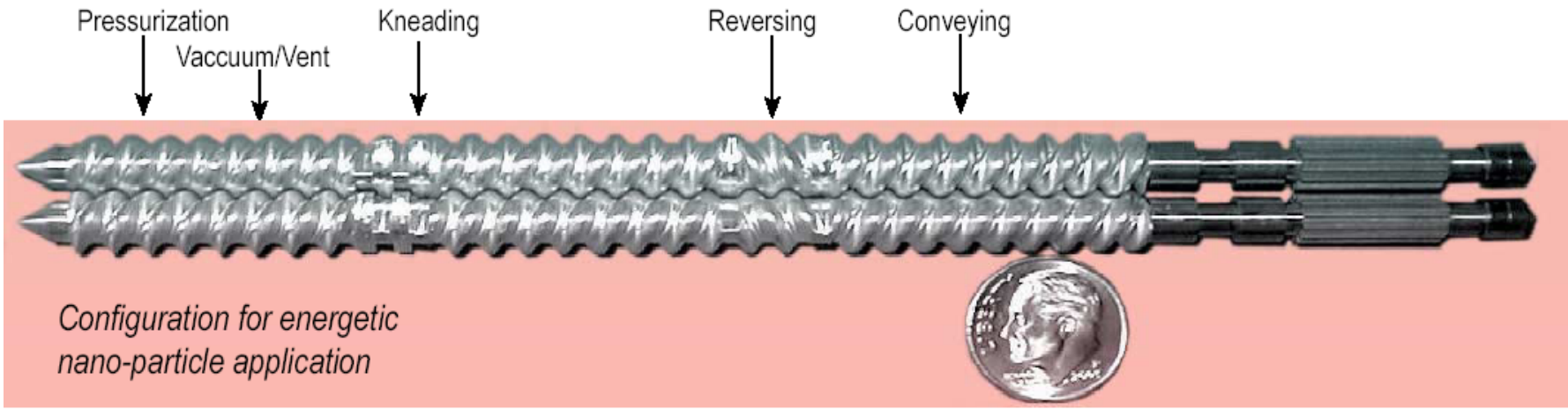
Pressurization
Vaccuum/Vent
Kneading
Reversing
Conveying
Configuration for energetic
nano-particle application

Figure 14

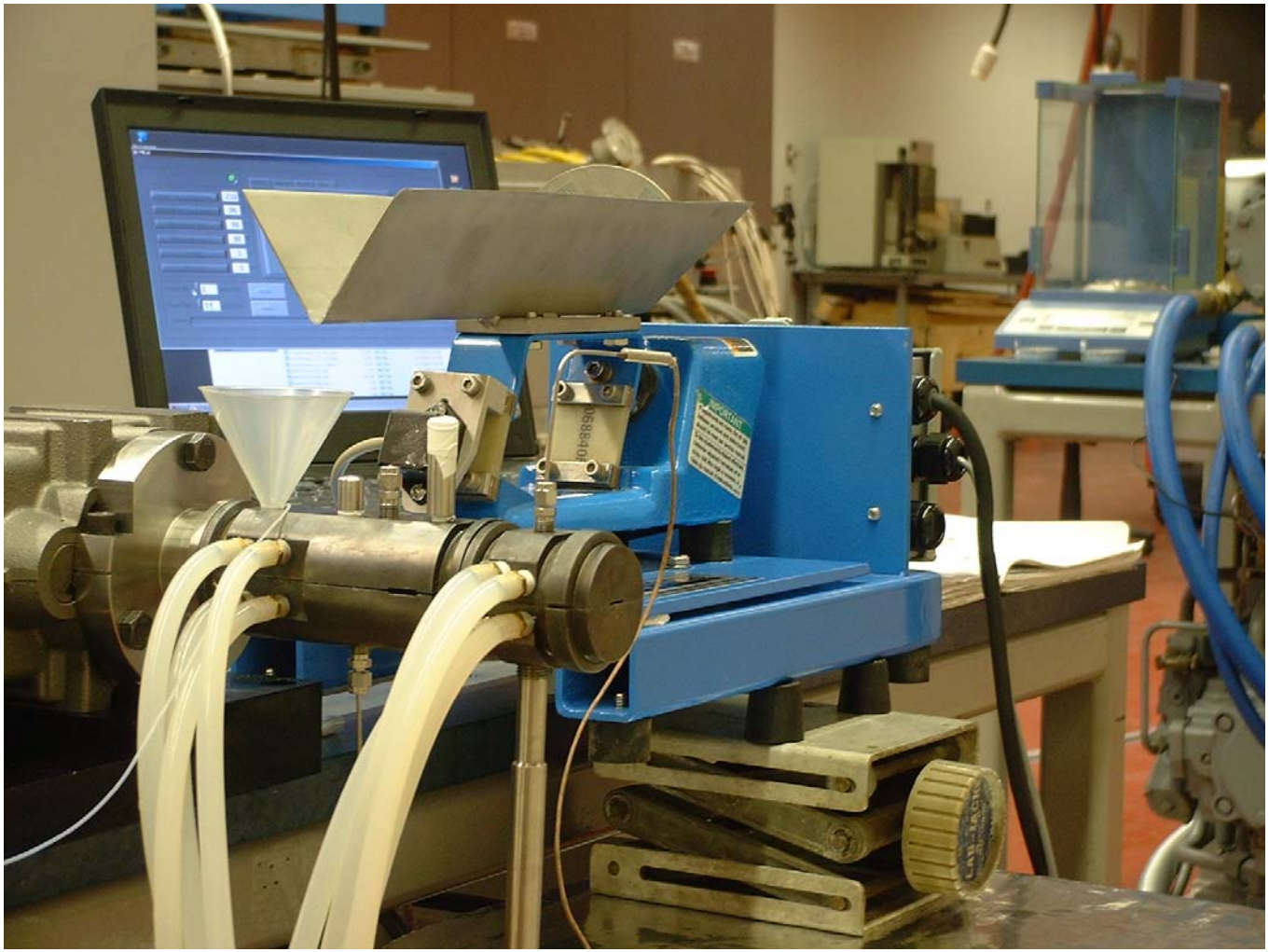

Figure 15

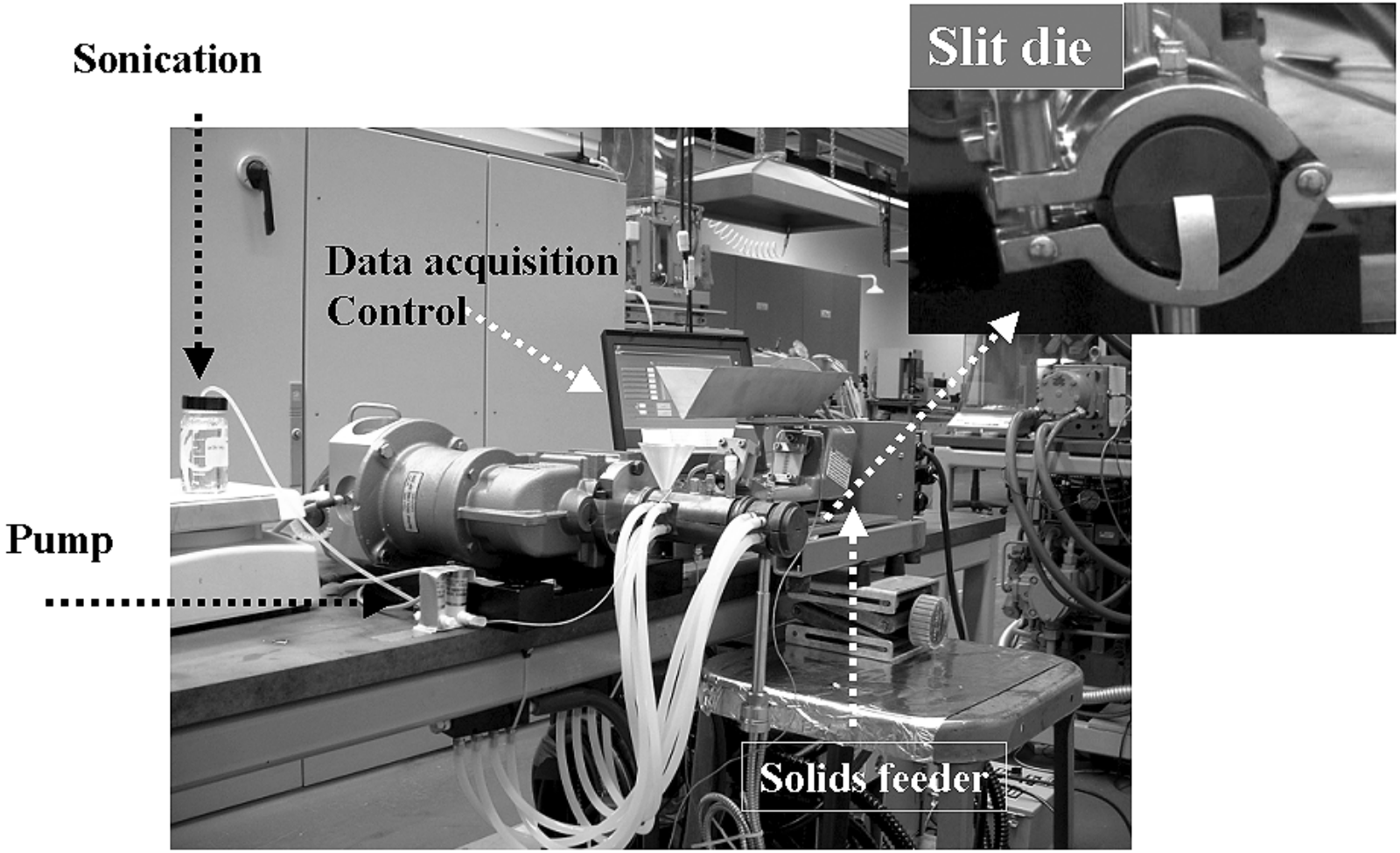

The auxiliaries of the twin screw extruder specifically designed and built for incorporating nanoparticles

Figure 16

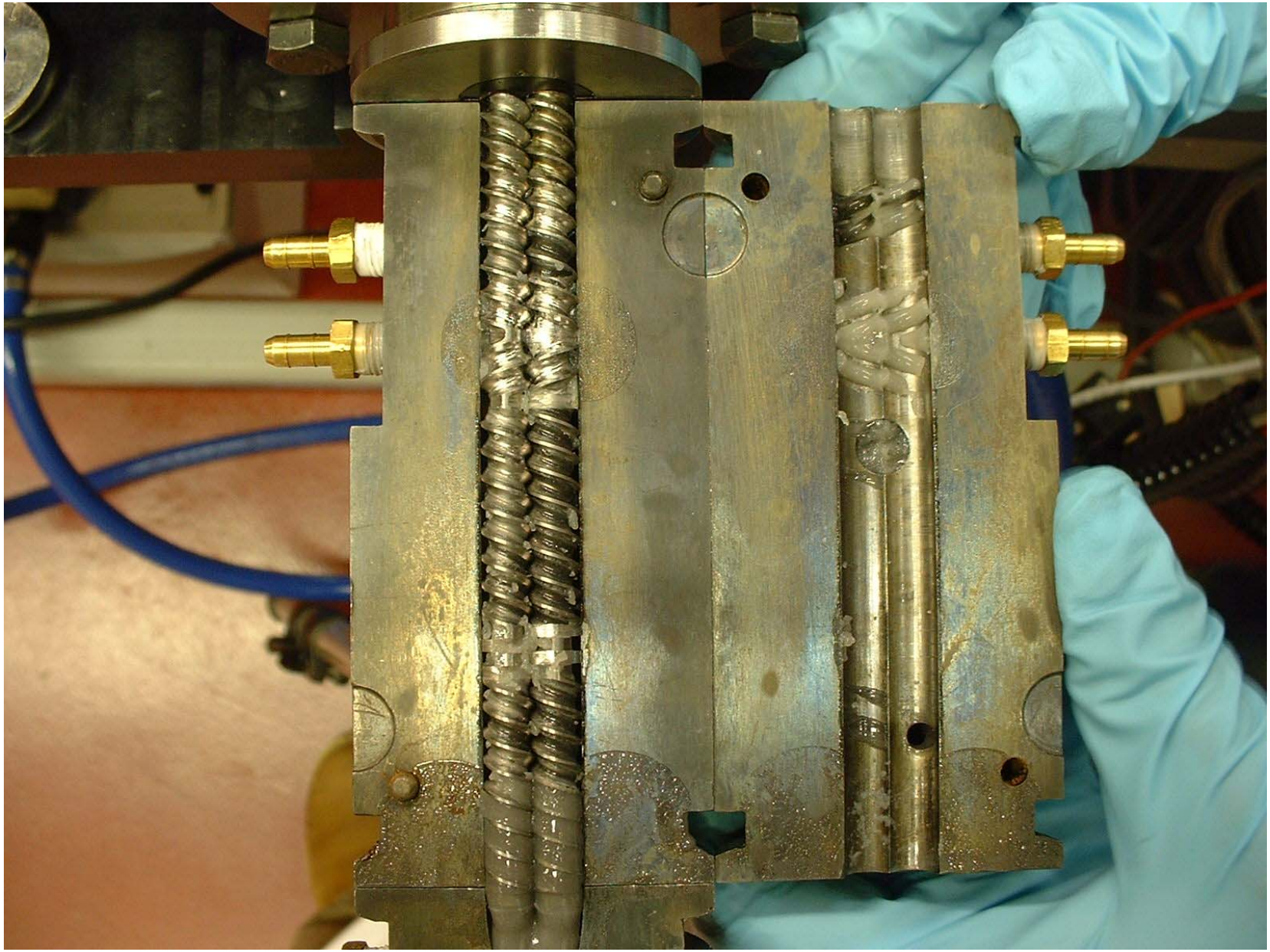

DEAD STOP at Q=21.98g/h, 150rpm, 435psi

Figure 17

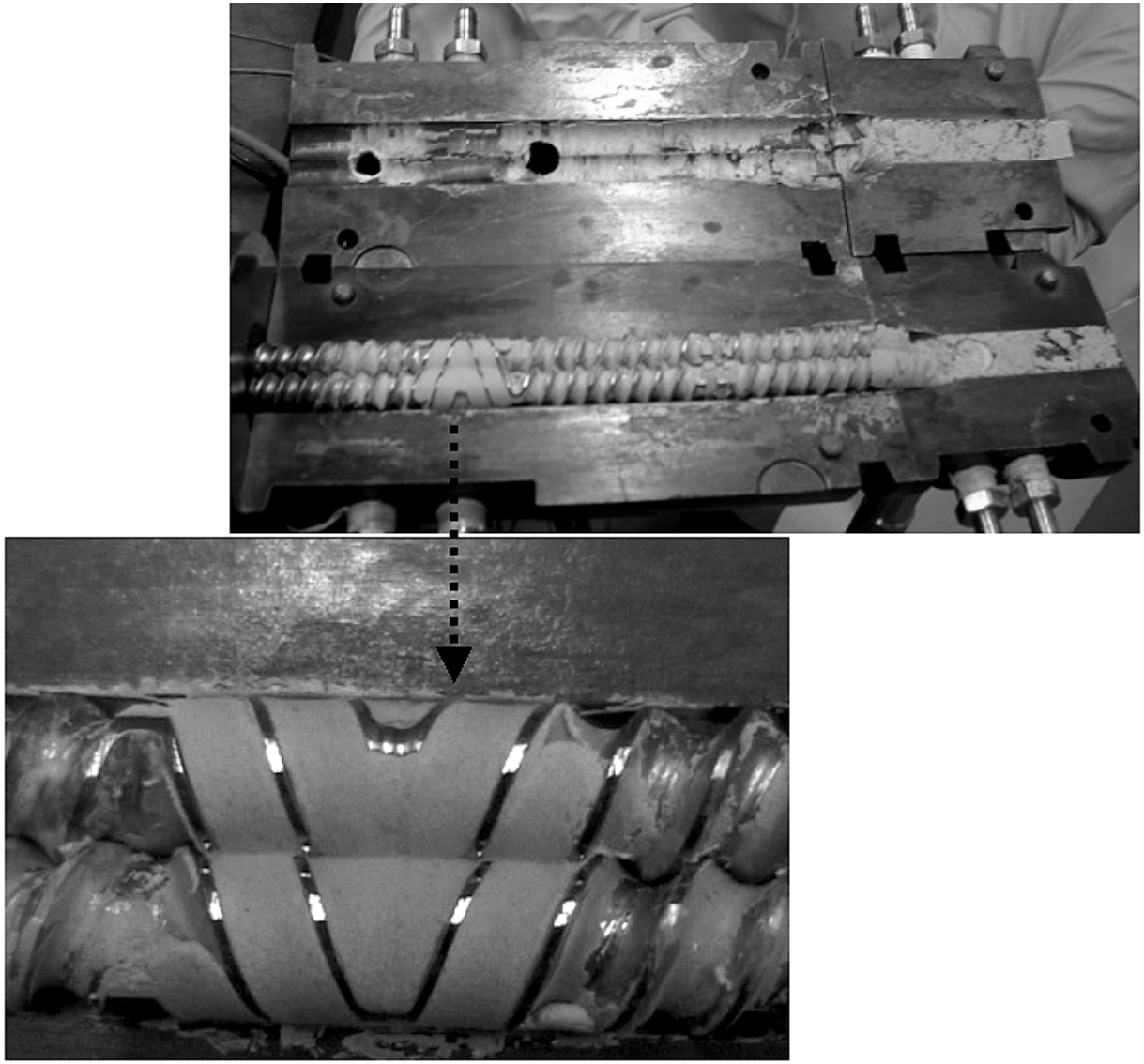

The typical degree of fill distributions in the twin screw extruder upon a dead stop.

Figure 18

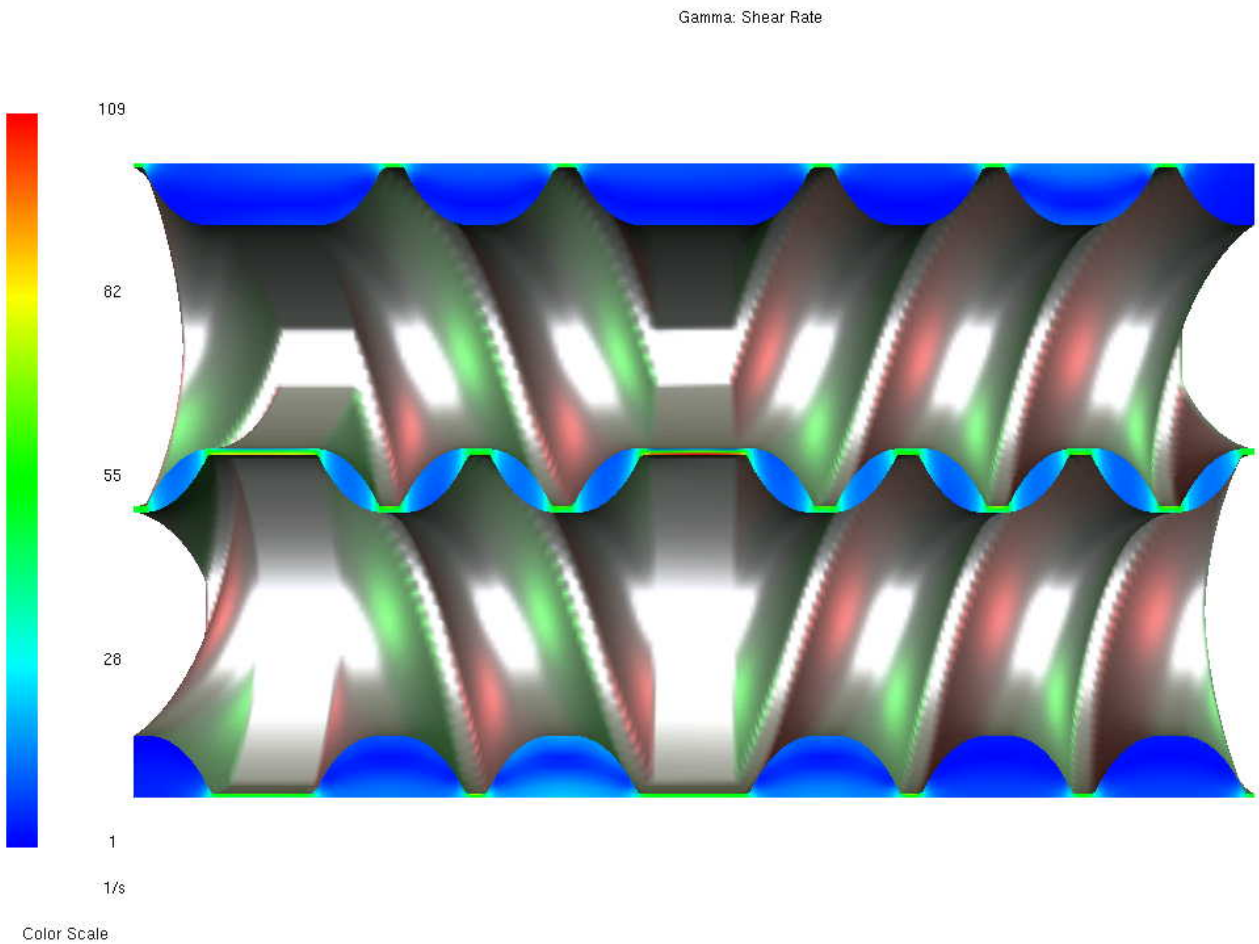

Mini Extruder First Section, 0.05 lb/hr, 105°C, τ_o = 0 Pa, m=80 Pa-s^n, n=1.0

Figure 19

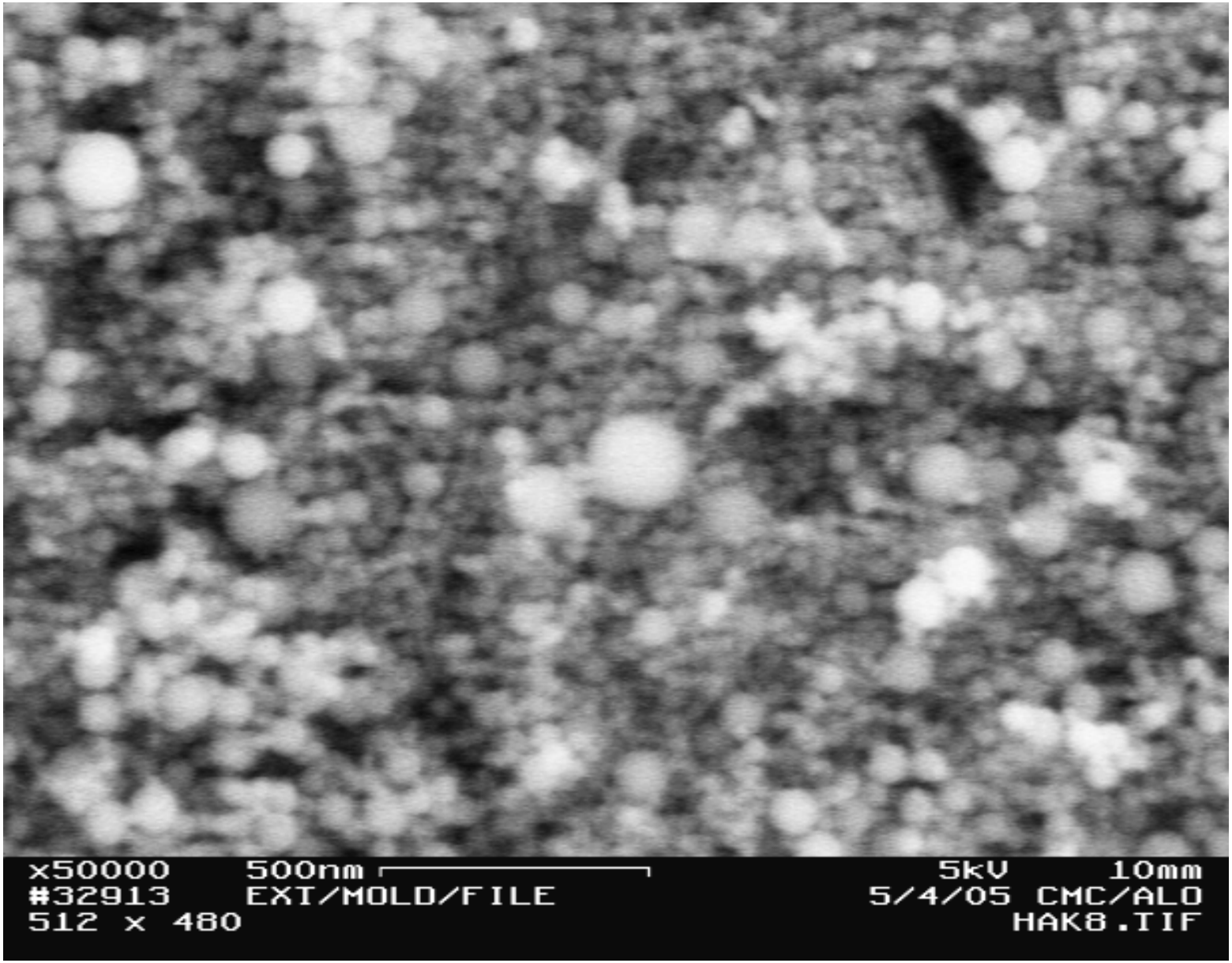

γ-Al_2O_3 Particles.

Figure 20

(Inframat Avanced Materials, LLC, CT., USA. Particle size 40nm)

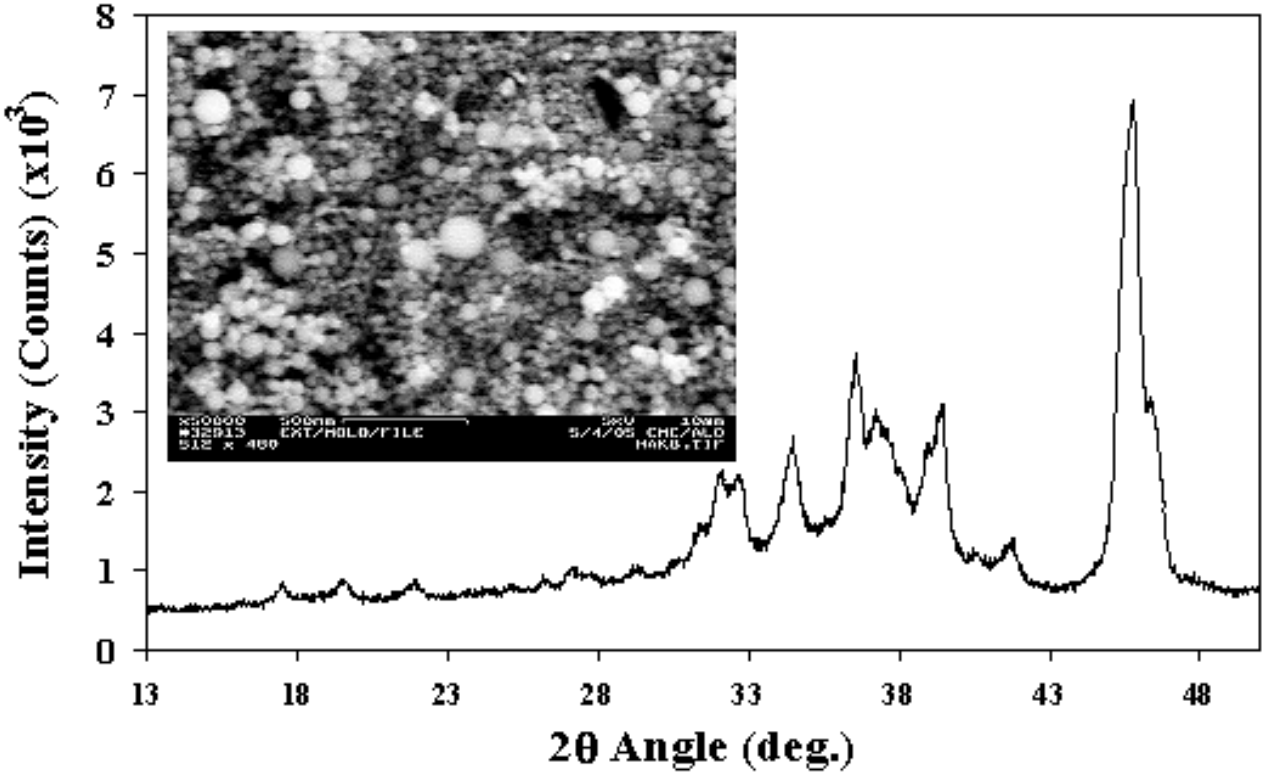

Sample name	Average 2 θ (degree)	Average FWHM	Average crystallite size t (nm)
Pure γ- Al_2O_3	45.746	0.659	13.59

The x-ray diffraction pattern and SEM micrograph of γ–Al_2O_3.

Figure 21

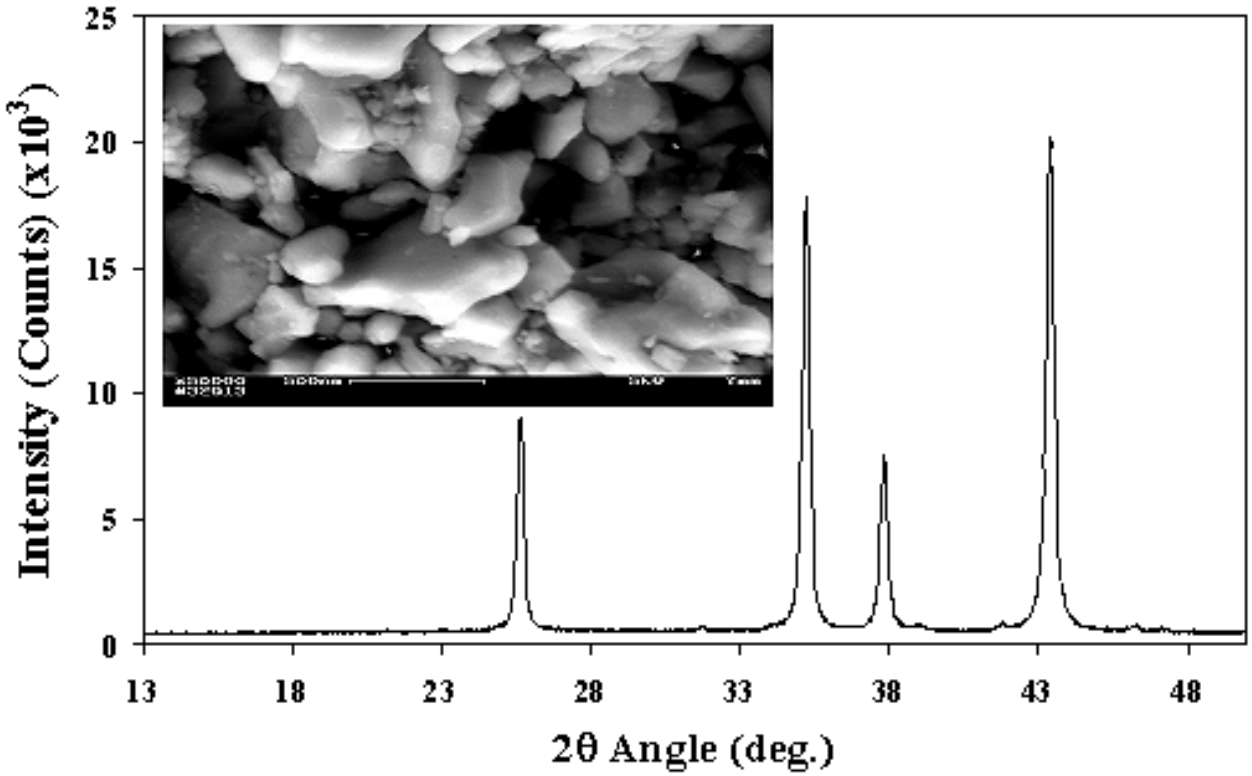

Sample name	Average 2 θ (degree)	Average FWHM	Average crystallite size t (nm)
Pure α- Al_2O_3	46.266	0.262	43.94

The x-ray diffraction pattern and SEM micrograph of $\alpha-Al_2O_3$. Figure 22

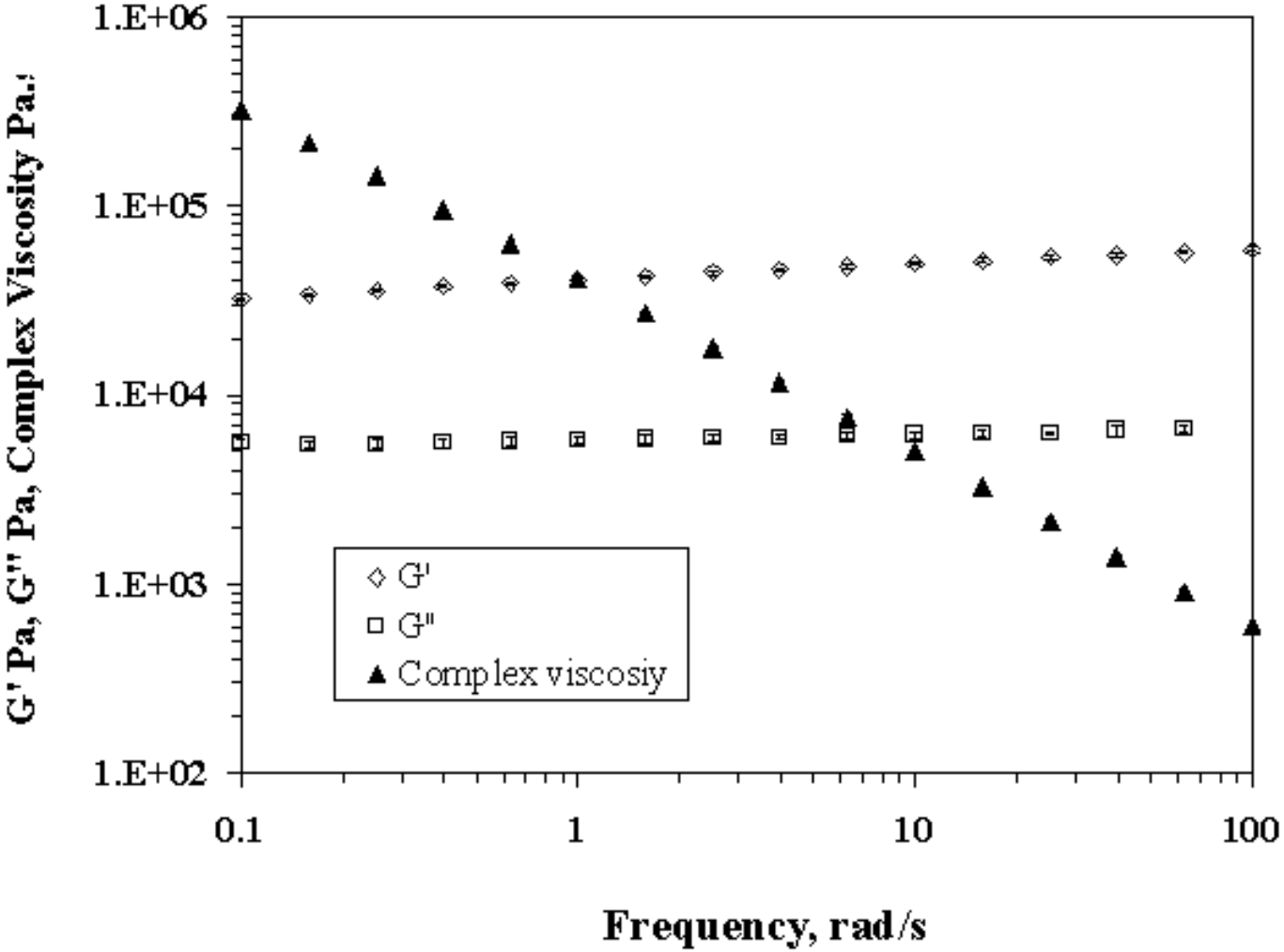

Typical dynamic properties of gel binder

Figure 23

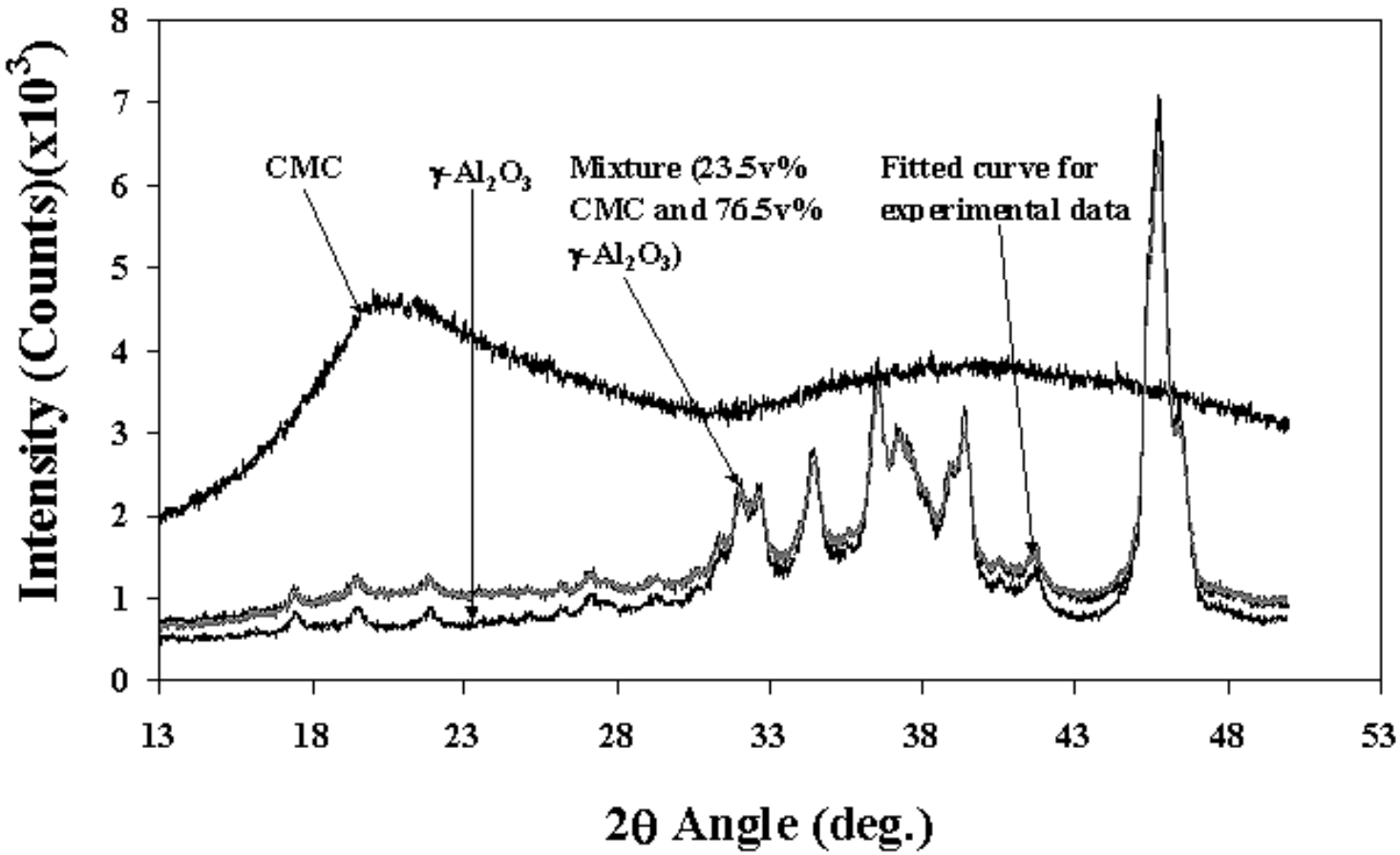

Typical x-ray diffraction patterns of the simulant formulation and its various ingredients.

Figure 24

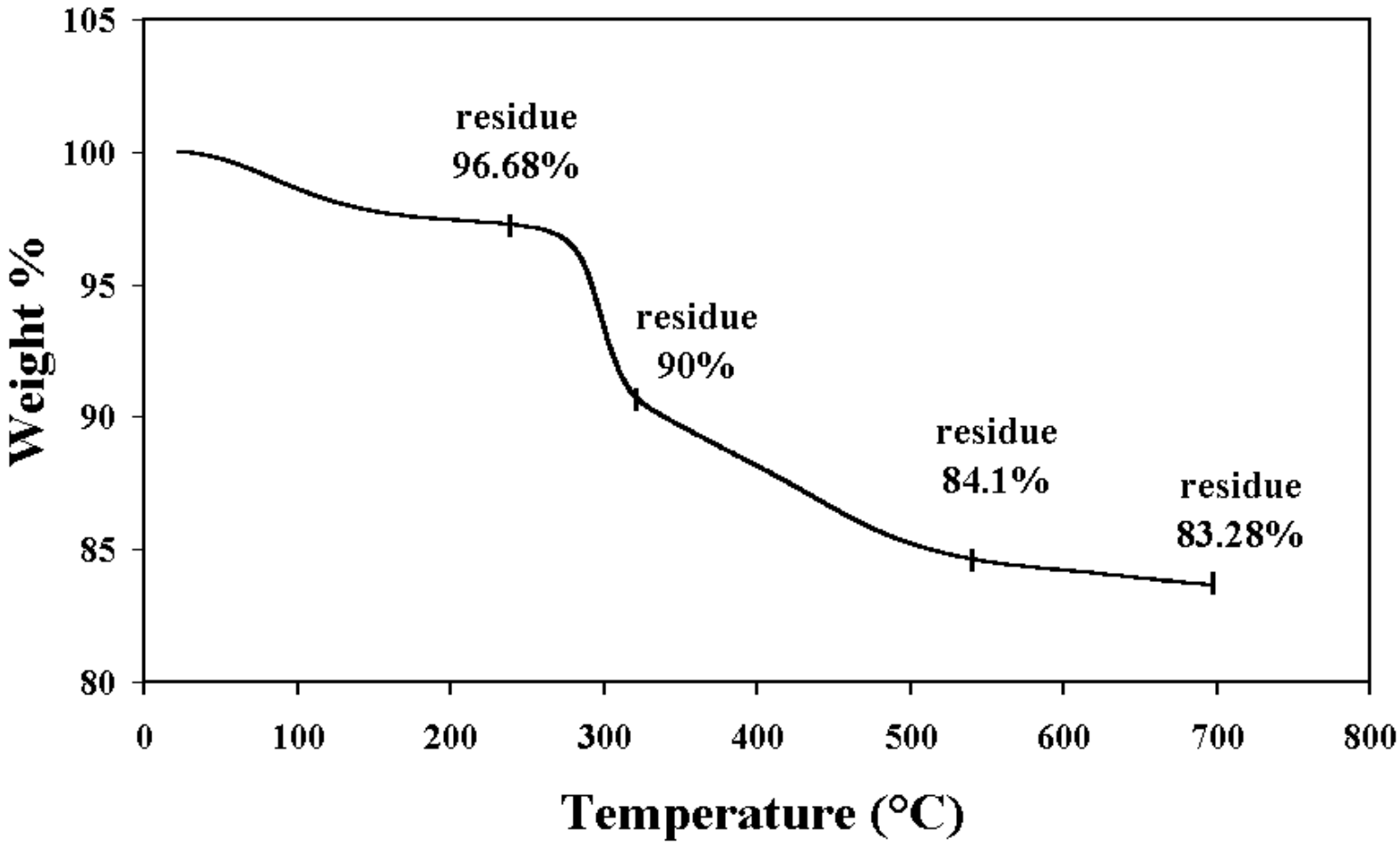

Typical thermo-gravimetric analysis results of the simulant formulation.

Figure 25

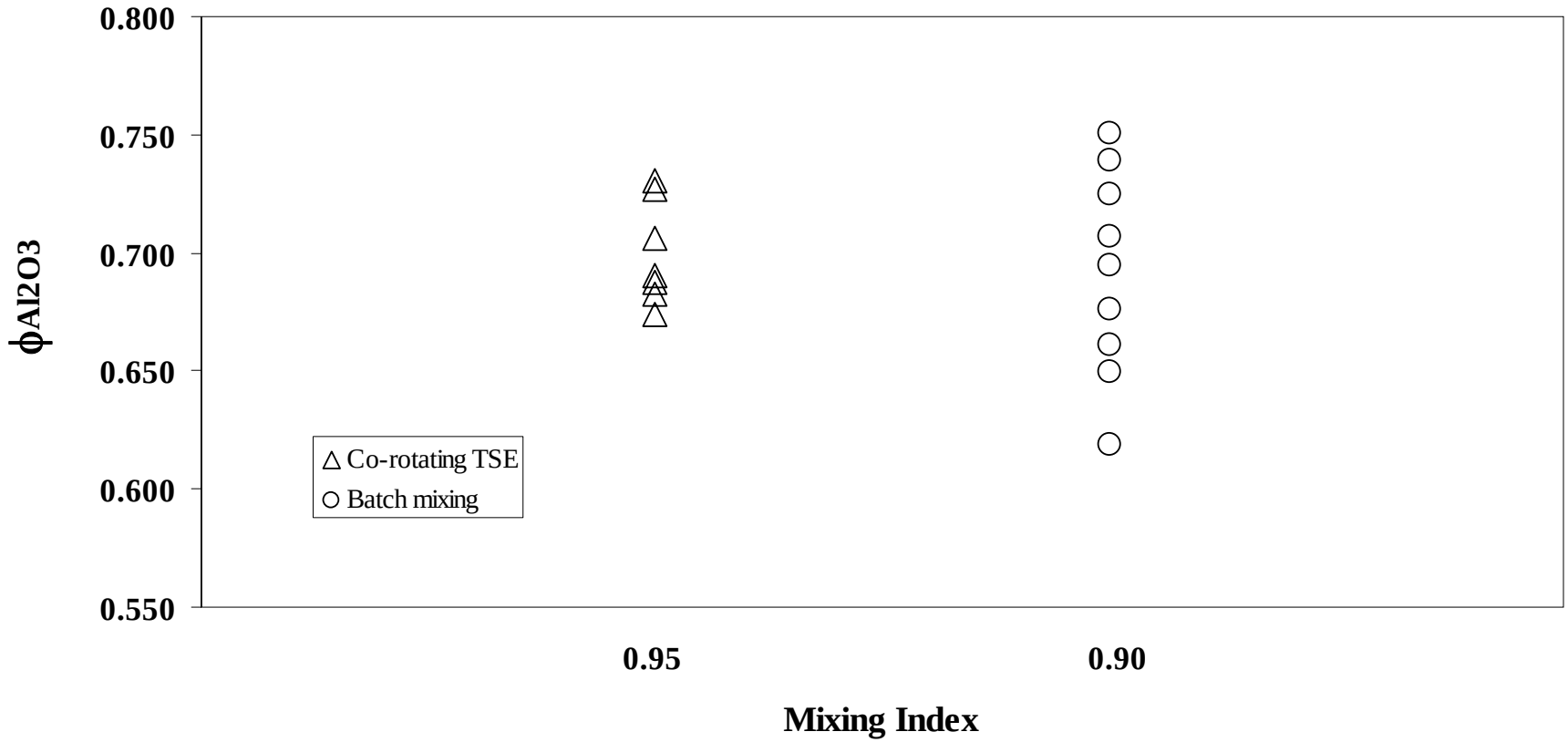

29%NaCMC+71% nano γ-Al_2O_3 **TGA** data,

Figure 26

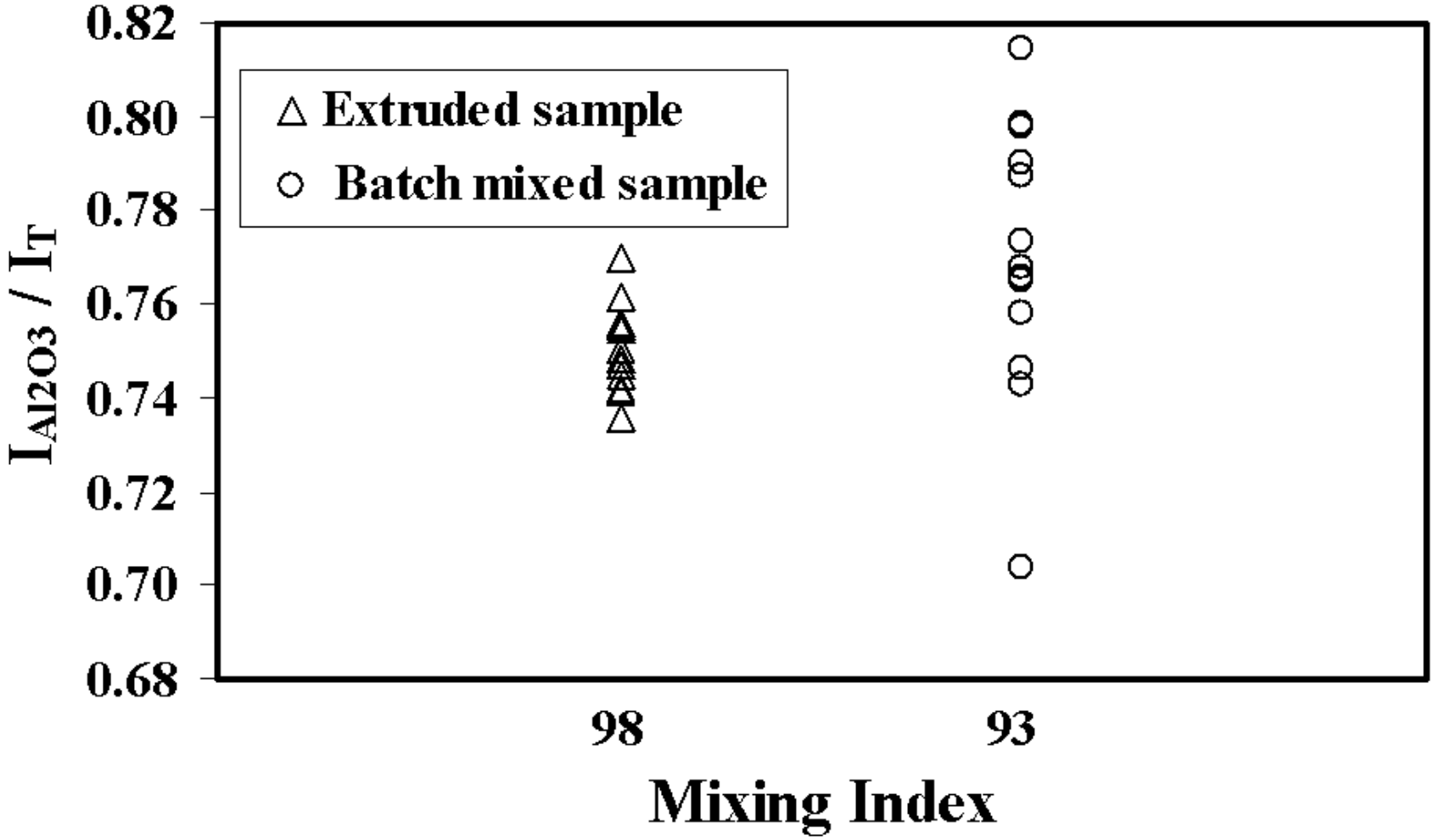

Scatter of the x-ray diffraction data for mixtures prepared with conventional and twin screw extrusion processes and their mixing indices

Figure 27

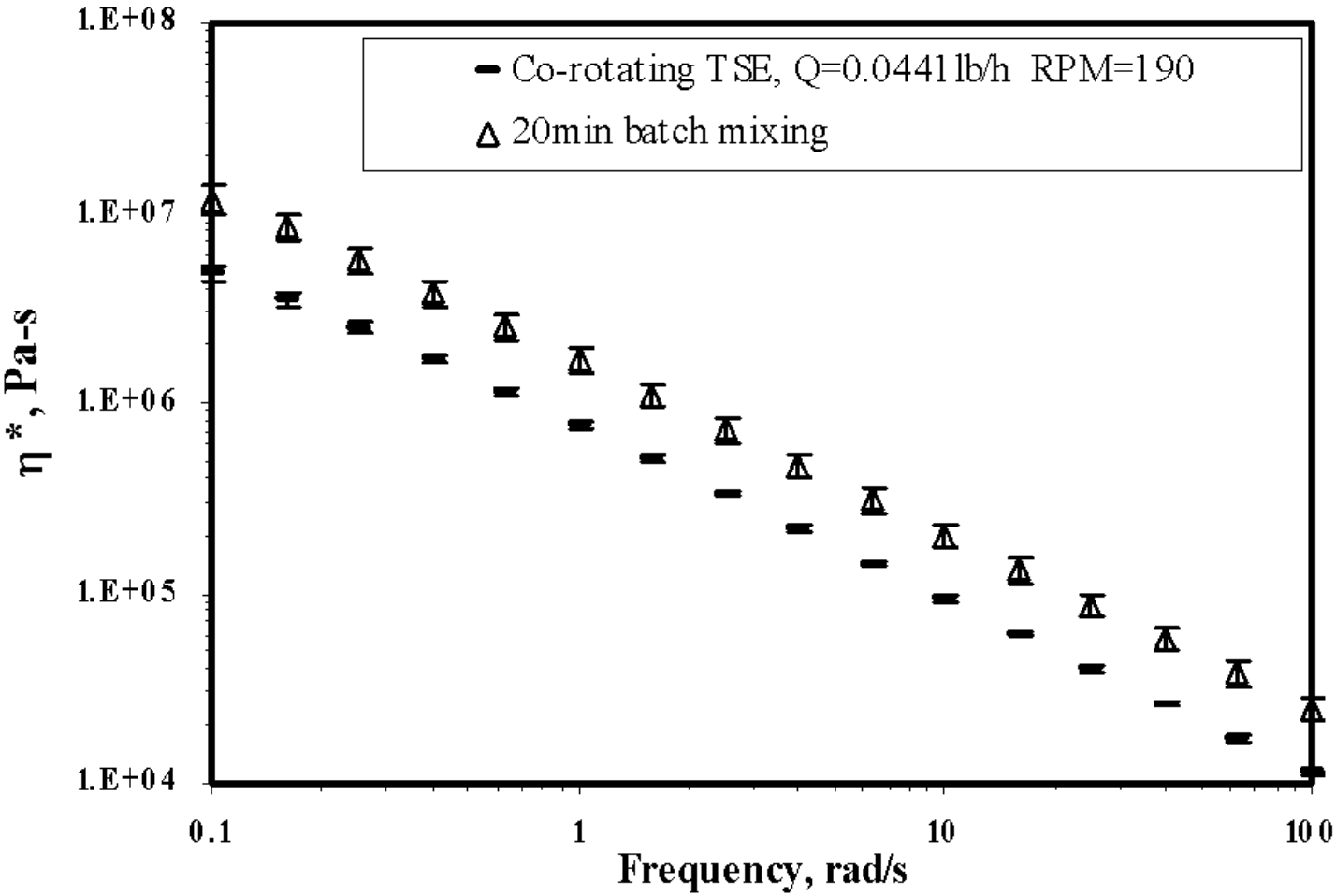

Confidence intervals of the magnitude of complex viscosity, η*, data for mixtures prepared with conventional and twin screw extrusion processes

Figure 28

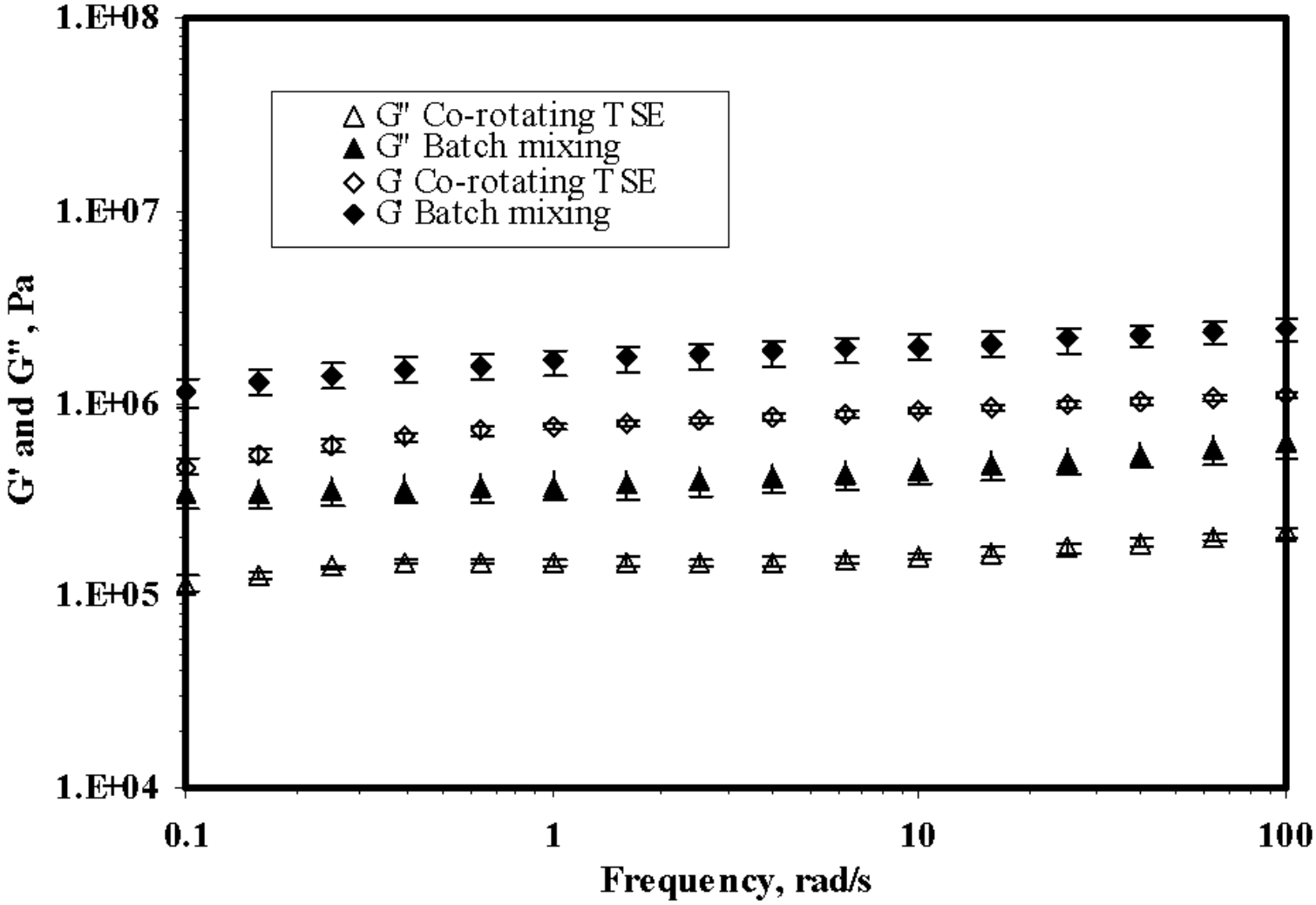

Confidence intervals of the storage modulus, G', and loss modulus, G", data for mixtures prepared with conventional and twin screw extrusion processes

Figure 29

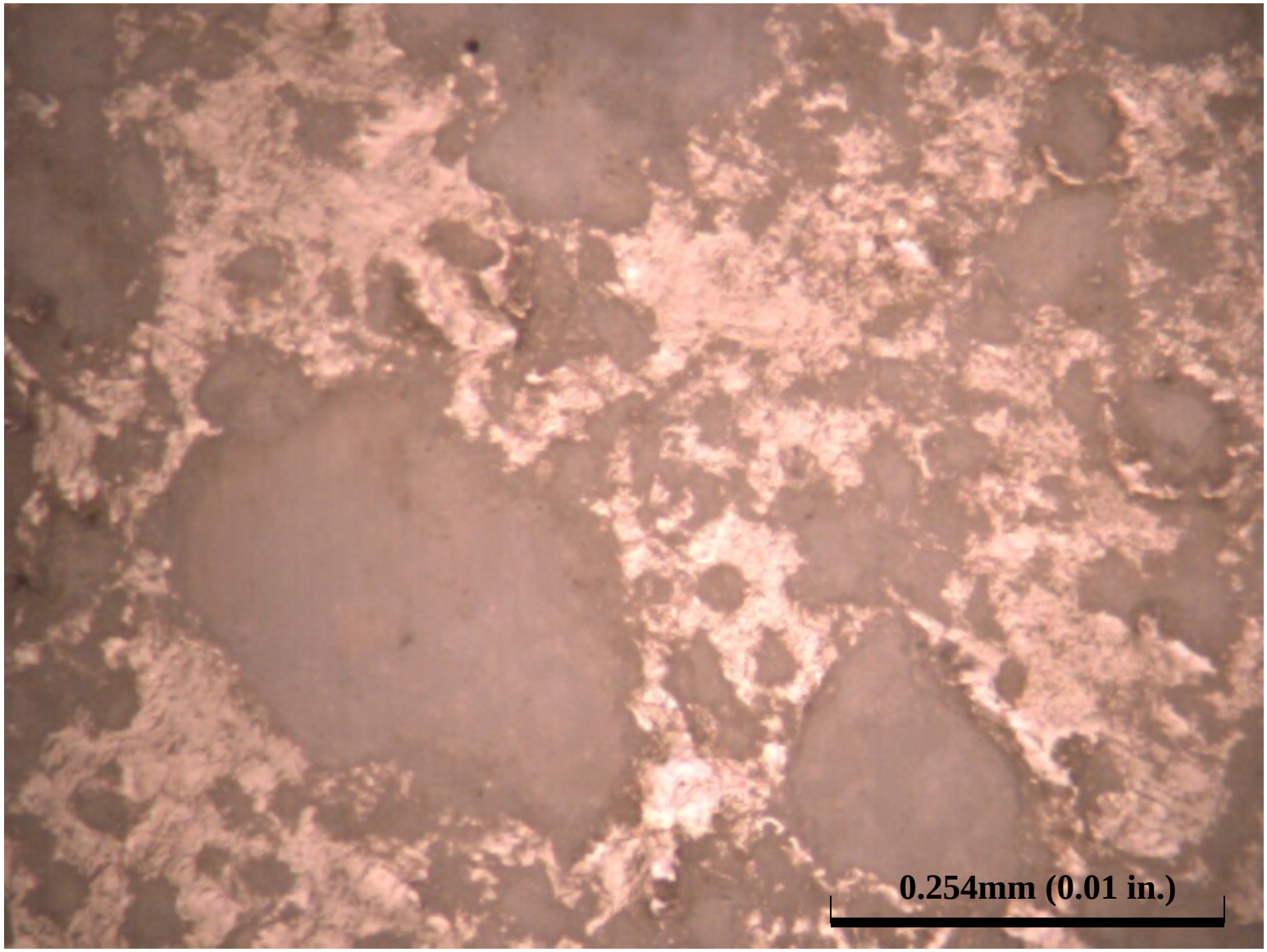

29%CMC+71% γ-Al_2O_3. Batch mixed and Air dried, file polished sample surface at 10x magnification.Optical microscope

Figure 30

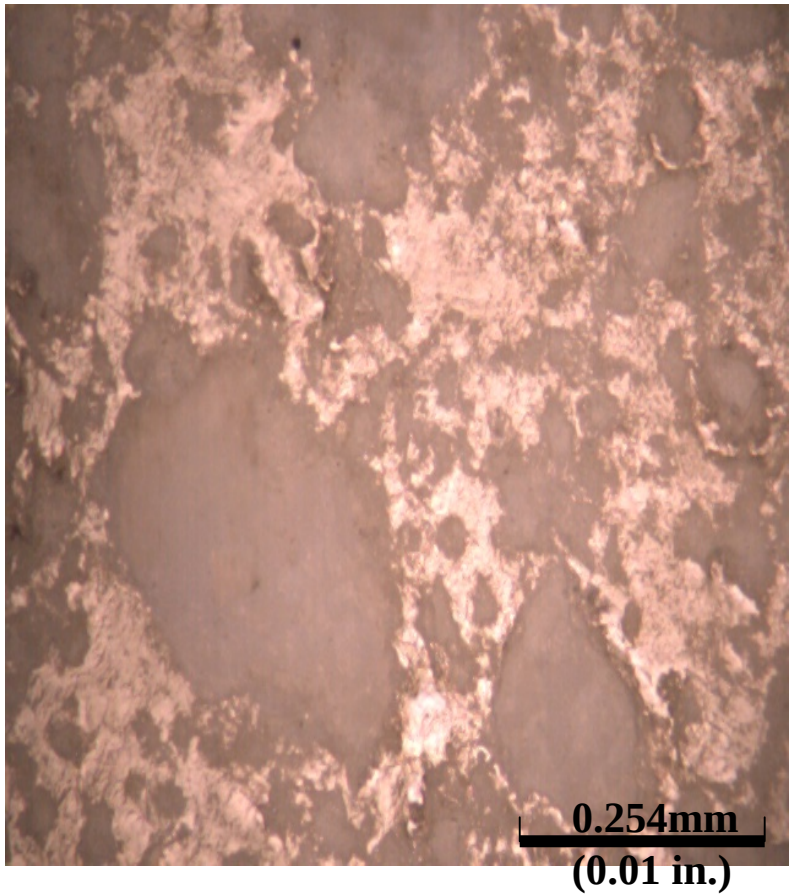

Batch mixed

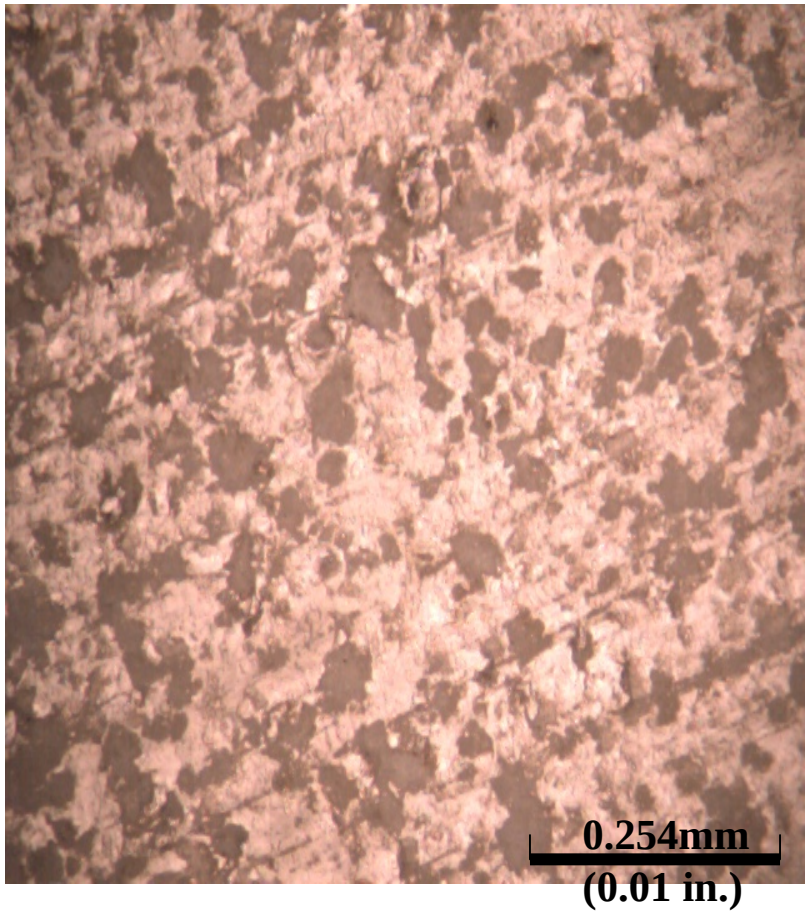

Twin screw extruded

Comparison of the mixing states from conventional intensive batch mixing versus twin screw extrusion.

Figure 31

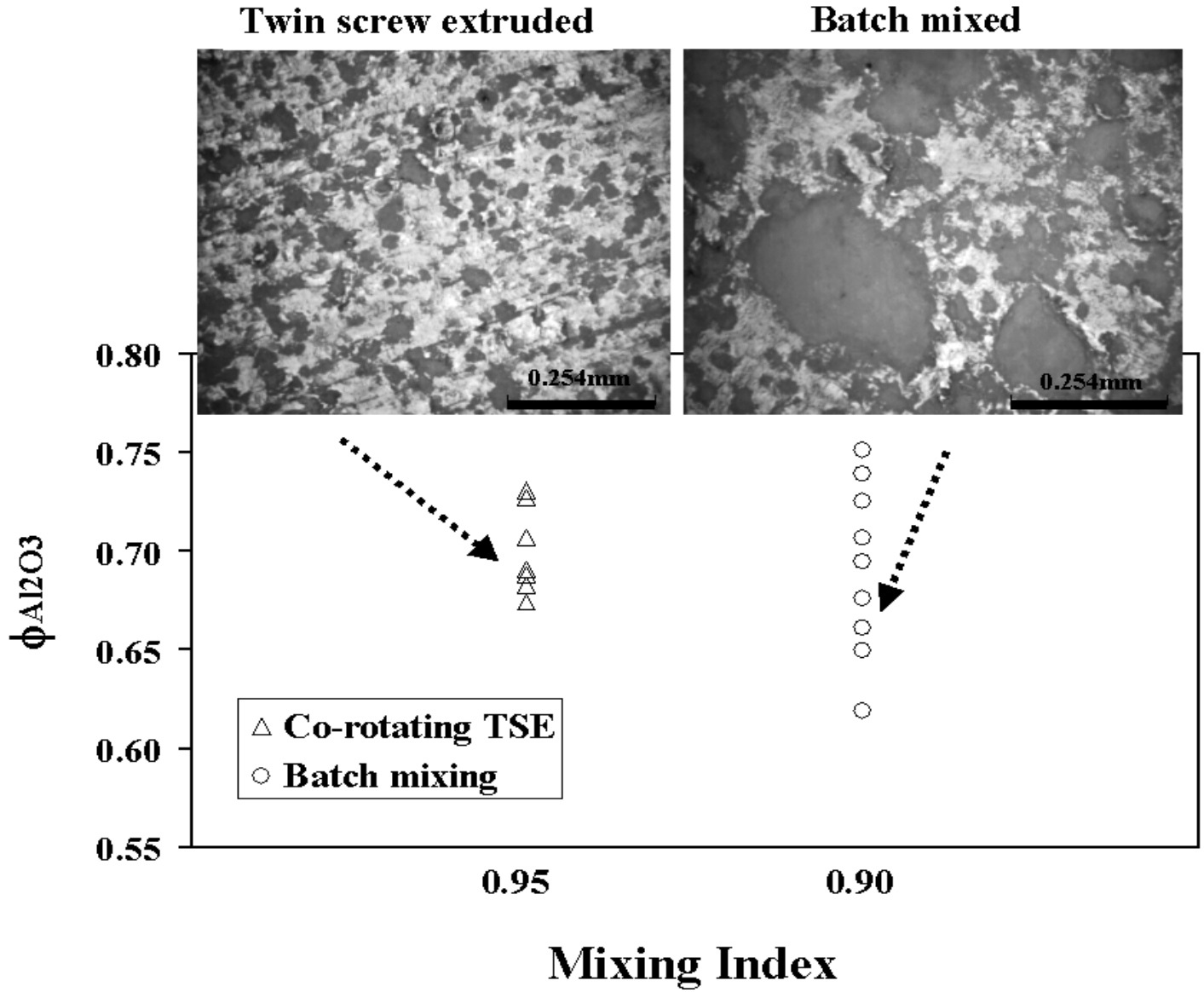

Scatter of the thermo-gravimetric analysis data for mixtures prepared with conventional and twin screw extrusion processes and their mixing indices

Figure 32

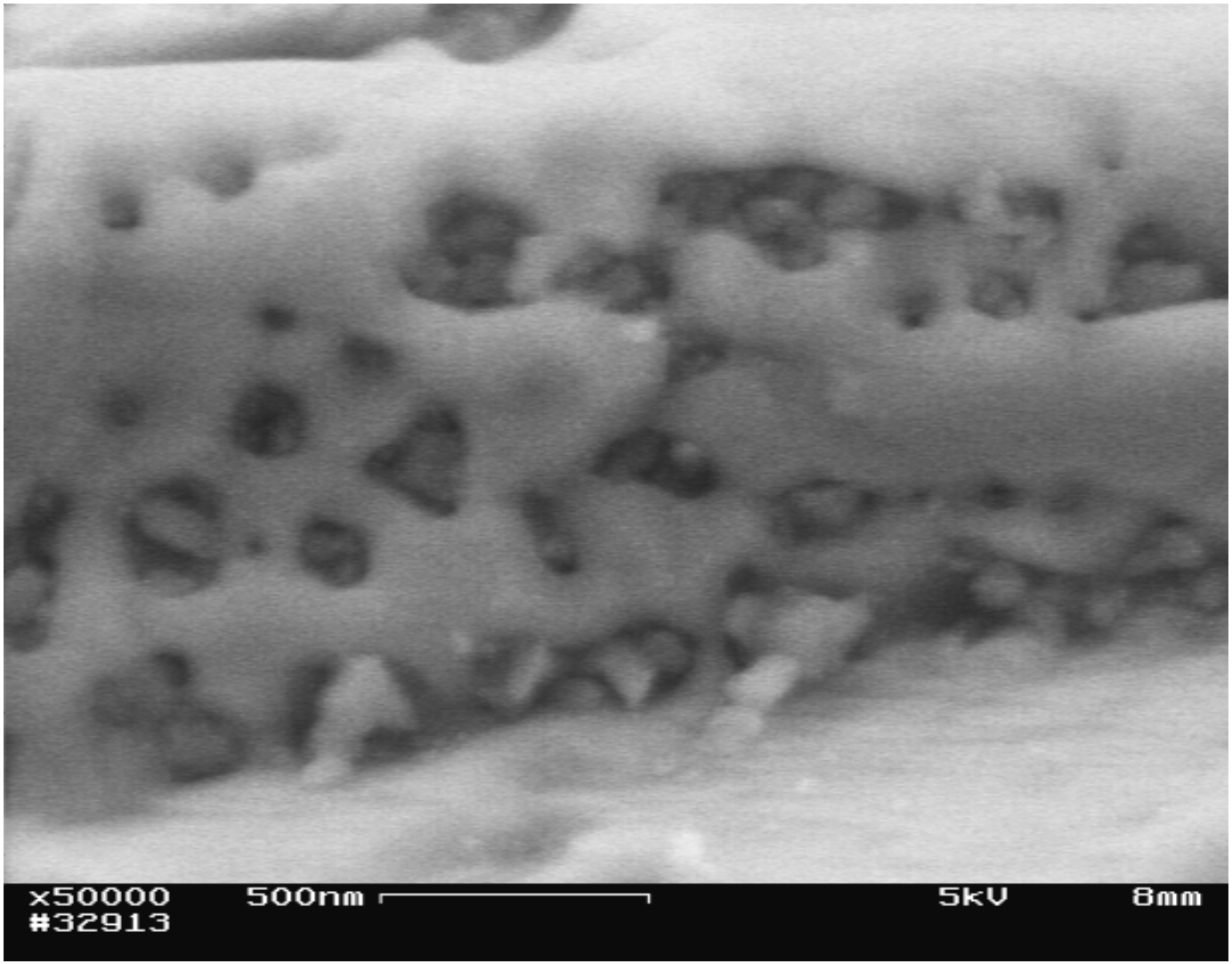

Typical scanning electron microscope, SEM, micrograph of batch mixed samples

Figure 33

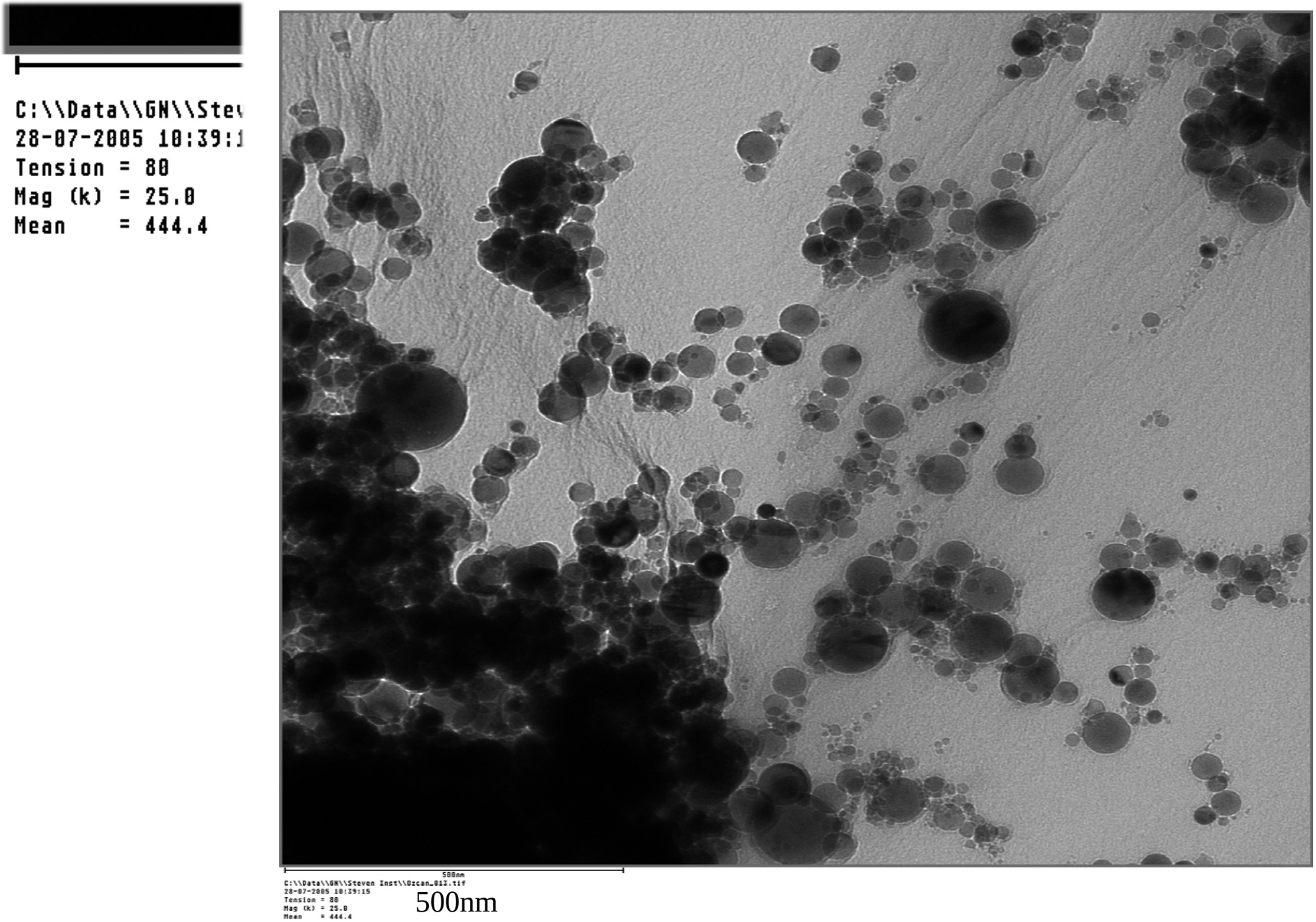
C:\\Data\\GN\\Ste
28-07-2005 10:39:1
Tension = 80
Mag (k) = 25.0
Mean = 444.4
500nm
C:\\Data\\GN\\Steven Inst\\Ozcan_013.tif
28-07-2005 10:39:15
Tension = 80
Mag (k) = 25.0
Mean = 444.4
500nm

Figure 34

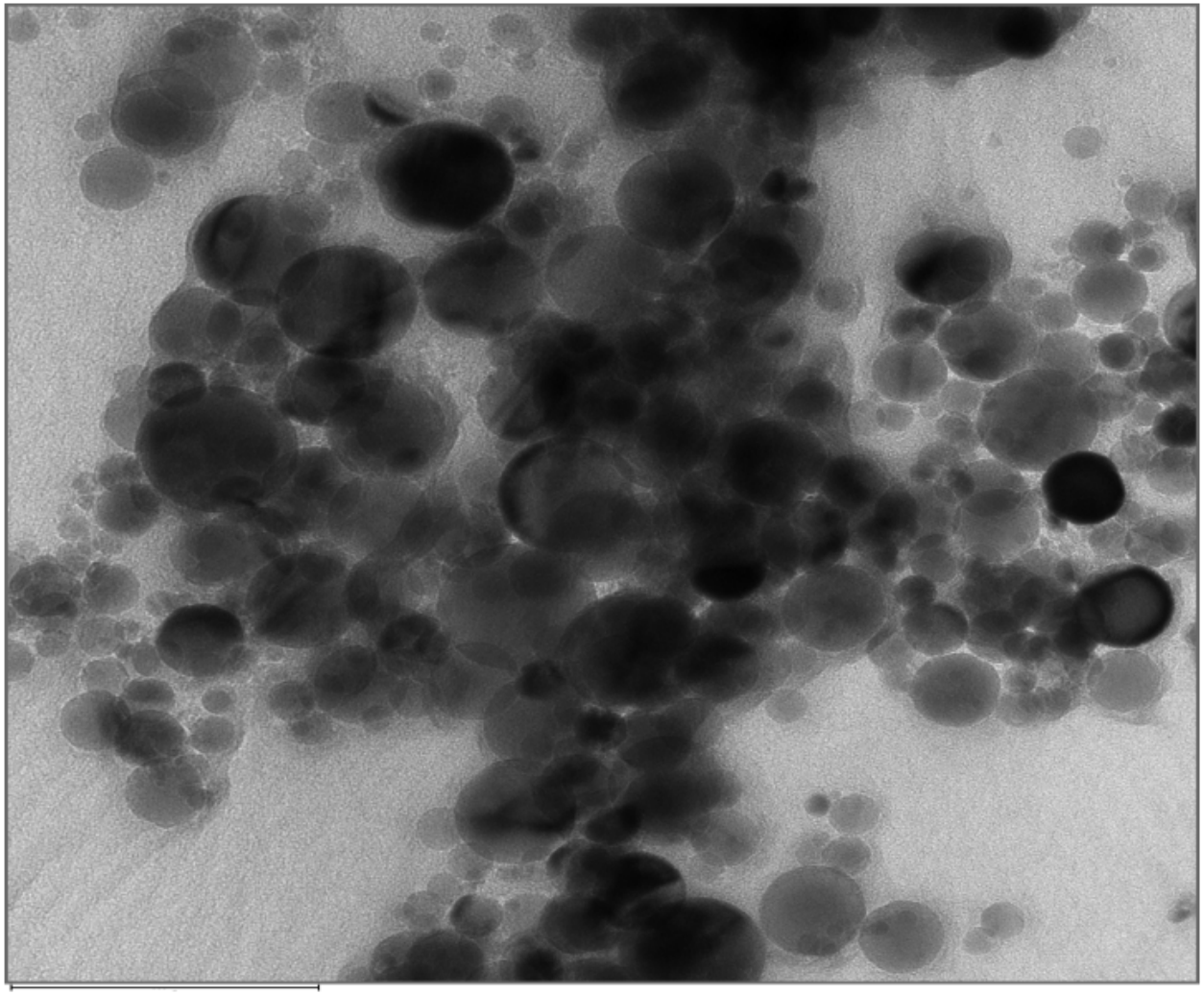

200nm

Typical transmission electron microscope, TEM, micrograph showing nanoparticle clusters

Figure 35

C:\\Data\\GN\\Ste
28-07-2005 10:40:
Tension = 80
Mag (k) = 50.0
Mean = 552.9

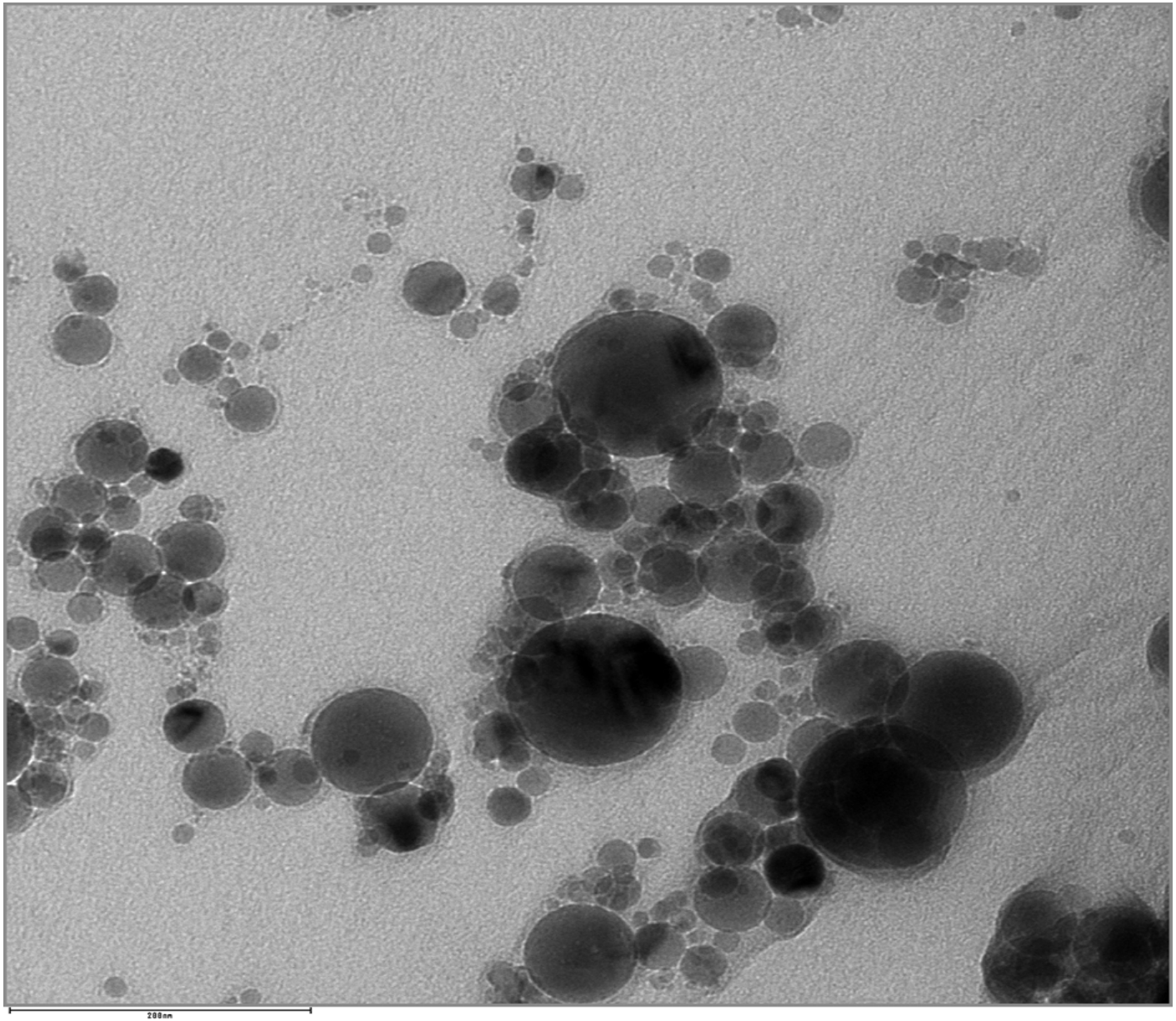

Figure 36

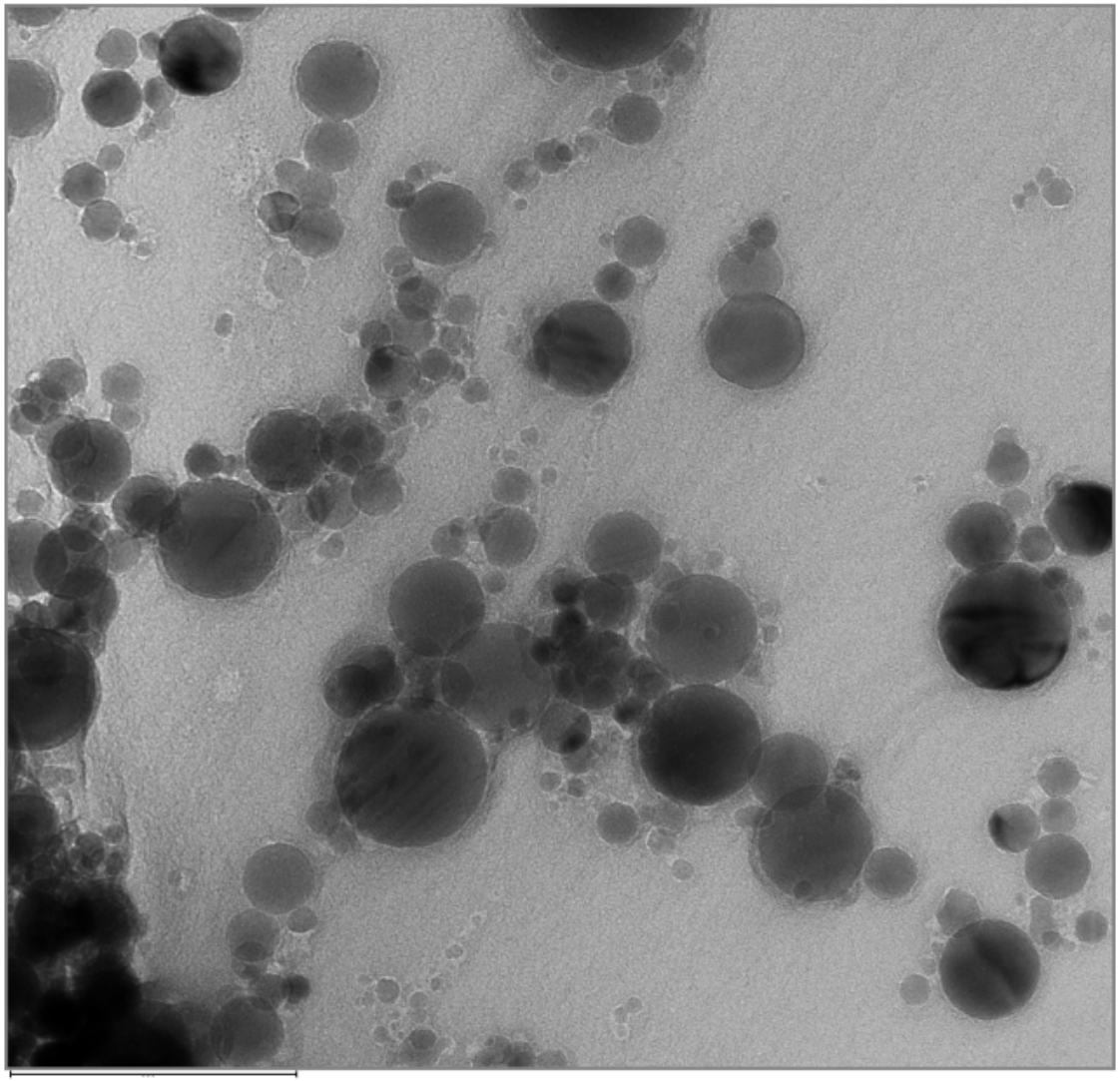

Typical transmission electron microscope, TEM, micrograph showing better dispersion of nanoparticles

Figure 37

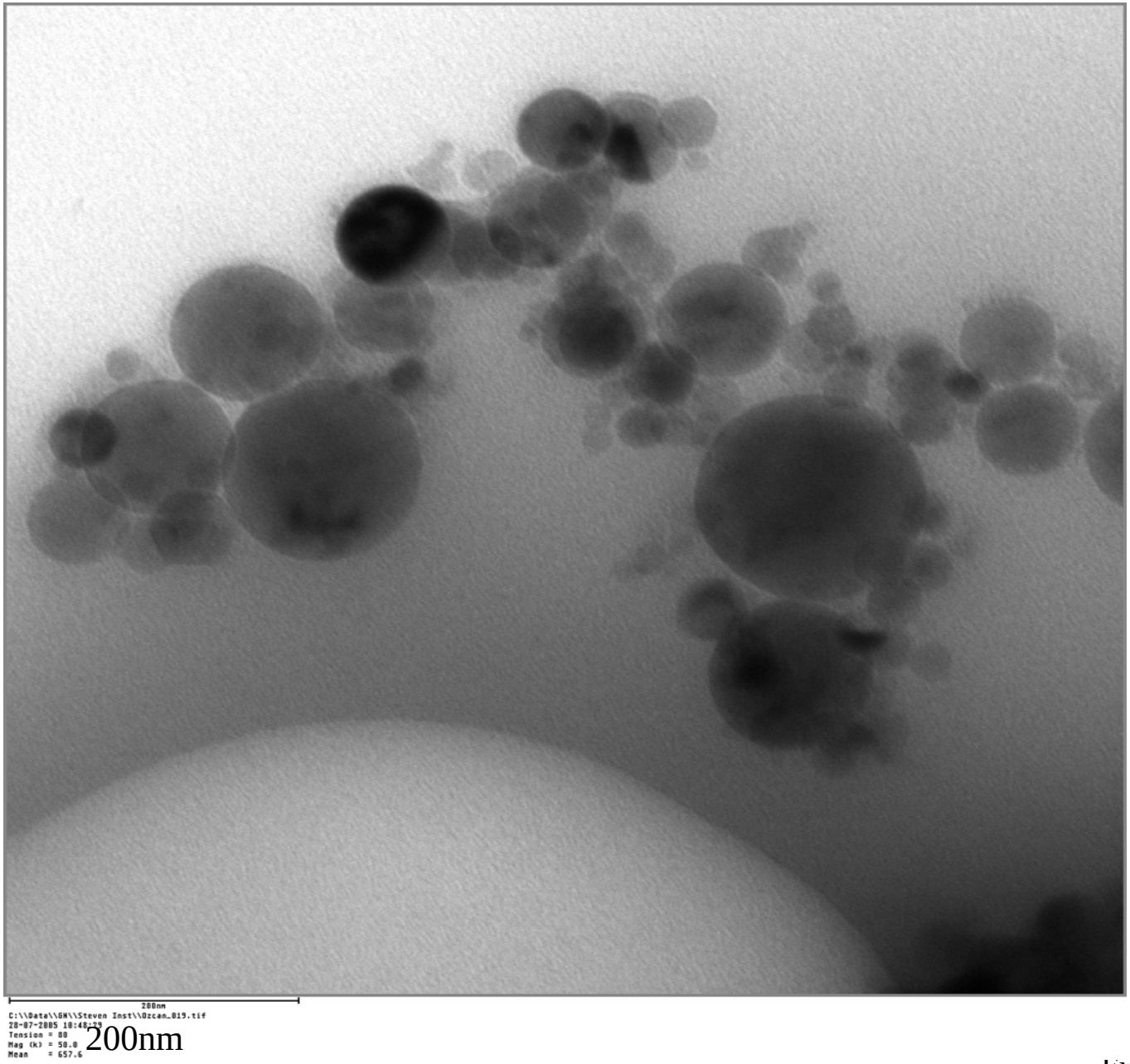
200nm
C:\\Data\\GN\\Steven Inst\\Ozcan_019.tif
28-07-2005 10:48:29
Tension = 80
Mag (K) = 50.0
Mean = 657.6
200nm

Figure 38

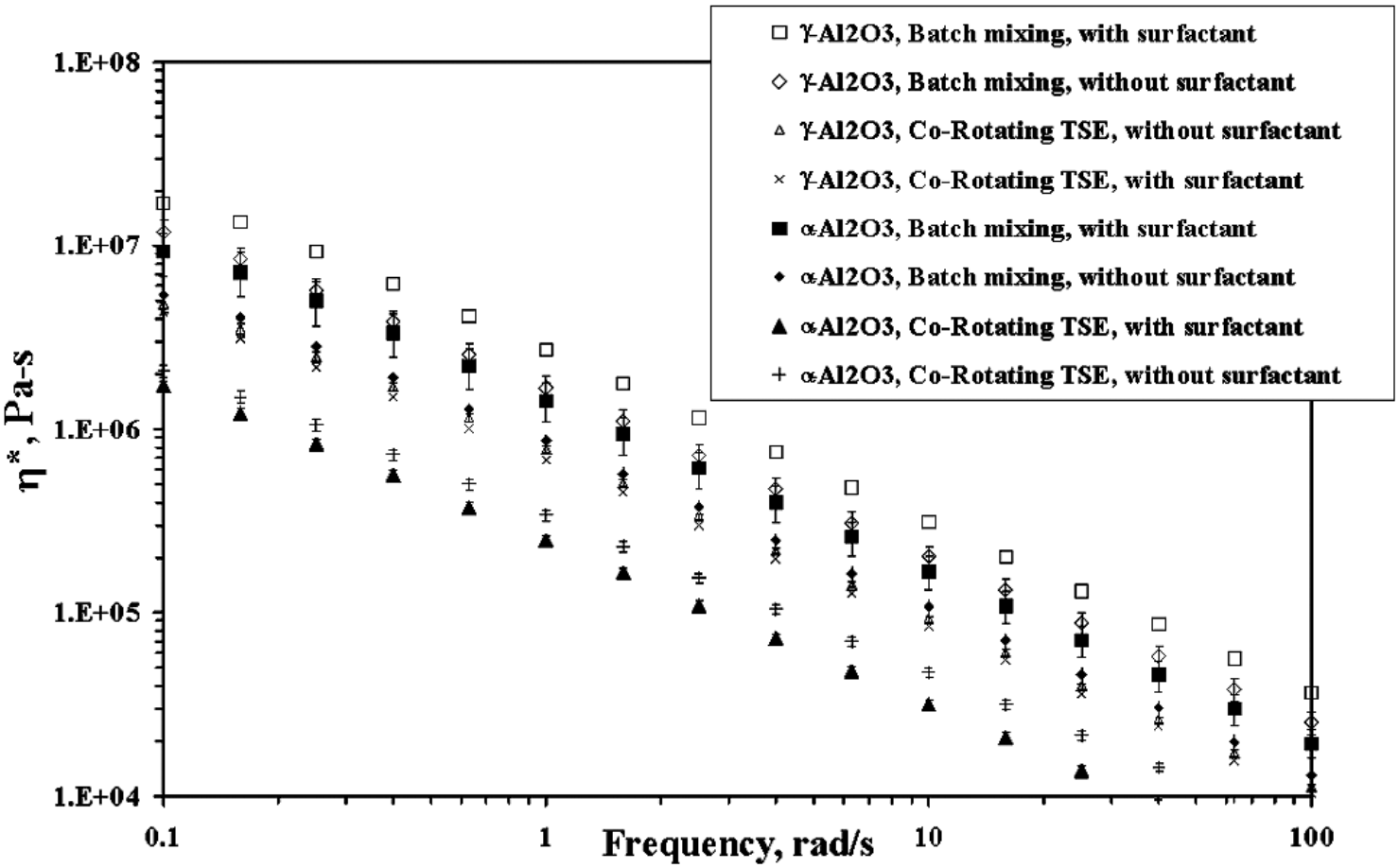

Typical magnitude of complex viscosity versus frequency data for suspensions prepared with or without the use of surfactants and processed with twin screw extrusion or conventional batch processing

Figure 39

Conclusions

- The ability to generate nanoenergetics depends on the interfacial interactions between the binder and the nanoparticles
- Without the correct chemistry nanoparticles remain as clusters and thus lose their core feature
- With the correct chemistry the proper selection of extruder geometry and operating conditions should allow adequate degree of mixing and particle size control.

Figure 40

The funding of US Army ARDEC under Contract DAAE30-02-BAA-0800 "Enabling Technologies for Manufacturing of Nanocomposites and Nanoenergetics" is gratefully acknowledged.

Figure 41